

$\nu = 1/2$ quantum Hall effect in the Aharonov-Casher geometry in a mesoscopic ring

R. Mélin* and B. Douçot†

CRTBT-CNRS, 38042 Grenoble BP 166X cédex France

Abstract

We study the effect of an electric charge in the middle of a ring of electrons in a magnetic field such as $\nu = 1/2$. In the absence of the central charge, a residual current should appear due to an Aharonov-Bohm effect. As the charge varies, periodic currents should appear in the ring. We evaluate the amplitude of these currents, as well as their period as the central charge varies. The presence of these currents should be a direct signature of the existence of a statistical gauge field in the $\nu = 1/2$ quantum Hall effect. Numerical diagonalizations for a small number of electrons on the sphere are also carried out. The numerical results up to 9 electrons are qualitatively consistent with the mean field picture.

*Present Address: International School for Advanced Studies (SISSA), Via Beirut 2-4, 34014 Trieste, Italy; e-mail: melin@crtbt.polycnrs-gre.fr

†Present address: LPTHE, Jussieu, tour 24-14, 4 place Jussieu, 75252 Paris Cedex France; e-mail: doucot@lpthe.jussieu.fr

1 Introduction

Recently, new experimental and theoretical developments have generated alternative viewpoints in the current understanding of the fractional quantum Hall effect. It seems the key idea is the notion of composite fermions, first introduced by Jain [1], which establishes a correspondence between the fractional quantum Hall effect at lowest Landau level filling $\nu = p/(2mp \pm 1)$ and the integer quantum Hall effect with p filled Landau levels. The mapping is achieved by attaching $2m$ flux quanta to each electron, which preserves fermionic statistics, and by first treating the statistical fluxes at the mean field level. This description has received considerable attention especially in the vicinity of $\nu = 1/2$. Experimentally, the system is characterized by a vanishing energy gap, and various physical properties strongly suggest the presence of a new Fermi liquid [2] in this problem. On the theoretical side, the composite picture with $m = 1$ has been advocated by Halperin, Lee and Read as a powerful microscopic basis to understand these Fermi liquid-like properties in the vicinity of $\nu = 1/2$ [3]. The vanishing of the gap for the sequence of states at $\nu = p/(2p \pm 1)$ as p goes to infinity receives for instance a very simple interpretation in this framework since the composite fermions experience an average flux equal to ϕ_0/p per particle, so the corresponding Landau level spacing goes as $1/p$. If the statistical gauge field fluctuations are taken into account, some complications arise since a logarithmic divergence of the effective mass as $p \rightarrow +\infty$ is predicted [3] [4]. There has been some trends in recent observation suggesting an effective mass enhancement [5] but this question is not settled yet. This theory has also been tested by numerical diagonalizations on finite systems [6] [7], and the composite fermion picture has been shown to predict for instance the right quantum numbers for the ground state and low-lying states [6], as well as the scaling of the ground state energy versus particle number [7]. Furthermore, a trial wave function inspired by these considerations provides a very good understanding of ground state correlations. We note however that this wave function is not merely the singular gauge transformation applied to the Slater determinant of composite fermions moving in zero external field, but it has to be improved by the combined effect of a short range Jastrow factor and a global projection on the lowest Landau level.

In this paper, we suggest a different test for the composite fermion approach. The basic idea is connected to the fact that if an external electric field generates a spatially dependent electronic density, the average flux acting on the composite fermions is no longer vanishing everywhere. We wish to detect such a variation of the effective flux. In the experiment we propose, local density fluctuations are created in a ring of $\nu = 1/2$ fermions, thanks to the presence of an electric charge localized in the middle of the ring. Due to the presence of this charge, the electrons have a trend to accumulate at the external edge of the ring if the central charge is negative, and to be repelled from the inner edge, which creates a non zero effective flux through the ring. A consequence of this non zero flux is the existence of observable persistent currents which vary periodically with the value of the charge in the center of the ring. At first glance, this phenomenon is reminiscent of the

Aharonov-Casher effect, which is expected to take place if a flux tube moves around a fixed charge [8]. This effect is a direct consequence of the Aharonov-Bohm effect and of Lorentz invariance, since the static electric field generated by the charge induces a non-vanishing magnetic field in the flux-tube co-moving frame. Experimentally, it has been observed with superconducting vortices in Josephson junction arrays [9]. However, we should emphasize here that the composite fermions do not carry the physical magnetic field which obeys Maxwell's equations, but rather a Chern-Simon flux, so the two situations are physically quite different.

This paper is organized as follows. We first sum up the formalism to deal with the mean field approach of the $\nu = 1/2$ quantum Hall effect. We then describe the geometry of the experiment, and propose a simplified geometry to get rid of the effects of curvature. In the absence of the central charge, one is able to solve exactly the eigenstates of the problem in the geometry of the experiment. In the presence of a central charge, the ring is electrically polarized. We propose a self consistent approach to find the electron density in the ring. Due to the presence of screening, the density fluctuations are localized in the vicinity of the edges of the ring. We finally obtain an order of magnitude for the average magnetic field through the ring. We calculate the current in the ring as a function of the central charge. We then present numerical computations of the effect on the sphere. After briefly writing the mean field theory on the sphere, we give numerical results for $\nu = 1/2$. A conclusion discusses the various results and mentions some open questions.

2 Mean field theory at $\nu = 1/2$

2.1 Gauge transformation at $\nu = 1/2$

We first sum up the mean field theory treatment of the half field Landau level [3]. It is possible to transform the original fermions in the magnetic field into new fermionic composite particles, with two flux quanta attached to them. The reason why attaching two flux quanta leads to fermions is that when one interchanges two particles with a flux ϕ attached to them, one gets a phase factor of $\exp i\theta$ in the wave function, with

$$\theta = \pi(1 + \frac{\phi}{\phi_0}), \quad (1)$$

where $\theta = \pi$ refers to fermionic particles. $\phi_0 = h/e$ is the flux quantum. The case $\phi = 2\phi_0$ thus corresponds to fermionic particles since in this case θ is π modulo 2π . The flux tubes are fixed via a non local gauge transformation, implemented in the following way. The second quantized form of the kinetic term in the Hamiltonian reads

$$\hat{K} = \frac{1}{2M} \int d^2\mathbf{x} \psi^\dagger(\mathbf{x}) (-i\hbar\nabla + e\mathbf{A}(x))^2 \psi(\mathbf{x}), \quad (2)$$

where M is the band electronic mass, e the absolute value of the electronic charge and $\psi^\dagger(\mathbf{x})$ the electronic field. The gauge transformation which realizes the passage from the electronic field $\psi^\dagger(\mathbf{x})$

to the composite fermionic field $\psi_C^+(\mathbf{x})$ is given by

$$\psi_C^+(\mathbf{x}) = \psi^+(\mathbf{x}) \exp \left\{ -2i \int d^2\mathbf{x}' \arg(\mathbf{x} - \mathbf{x}') \hat{\rho}(\mathbf{x}') \right\} \quad (3)$$

where

$$\hat{\rho}(\mathbf{x}) = \psi^+(\mathbf{x})\psi(\mathbf{x}) = \psi_C^+(\mathbf{x})\psi_C(\mathbf{x}) = \hat{\rho}_C(\mathbf{x}), \quad (4)$$

and $\arg(\mathbf{x} - \mathbf{x}')$ is the angle between the vector $\mathbf{x} - \mathbf{x}'$ and the x axis. The factor 2 in the exponential of (3) stands for two flux tubes attached to the electrons to form the composite fermions. In terms of the composite fermions, the kinetic energy reads

$$\hat{K} = \frac{\hbar^2}{2M} \int d\mathbf{x} \psi_C^+(\mathbf{x}) (-i\nabla + \frac{e}{\hbar} \mathbf{A}(\mathbf{x}) - \mathbf{a}(\mathbf{x}))^2 \psi_C(\mathbf{x}), \quad (5)$$

where the statistical gauge field is

$$\mathbf{a}(x) = 2 \int d\mathbf{x}' \frac{\hat{\mathbf{z}} \wedge (\mathbf{x} - \mathbf{x}')}{|\mathbf{x} - \mathbf{x}'|^2} \hat{\rho}_C(\mathbf{x}'). \quad (6)$$

The interaction term is

$$\hat{V} = \frac{1}{2} \int d\mathbf{x} d\mathbf{x}' v(\mathbf{x} - \mathbf{x}') : \hat{\rho}(\mathbf{x}) \hat{\rho}(\mathbf{x}') : = \frac{1}{2} \int d\mathbf{x} d\mathbf{x}' v(\mathbf{x} - \mathbf{x}') : \hat{\rho}_C(\mathbf{x}) \hat{\rho}_C(\mathbf{x}') :, \quad (7)$$

$v(\mathbf{x})$ being the Coulomb interaction

$$v(\mathbf{x}) = \frac{e^2}{4\pi\epsilon_0\epsilon_r|\mathbf{x}|}, \quad (8)$$

where ϵ_r is the relative dielectric constant of the material. For GaAs, $\epsilon_r = 12.6$.

2.2 Mean field theory

In the mean field theory approach, the density of fermions $\rho(\mathbf{x})$ is assumed to be constant. Since the average density n_0 is related to the field by the condition of half filling

$$n_0 = \frac{B}{2\phi_0}, \quad (9)$$

the mean field value of the statistical flux exactly cancels the external magnetic flux, and gives a zero residual magnetic field. The Hamiltonian of the system of composite fermions is simply the Hamiltonian of a collection of free fermions, but with a renormalized effective mass M^*

$$\hat{H}_{M.F.} = \frac{1}{2M^*} \int \psi^+(\mathbf{x}) (-i\hbar\nabla)^2 \psi(\mathbf{x}) d\mathbf{x} + \hat{V}. \quad (10)$$

If $B = 10T$, the value of the effective mass for GaAs is $M^* \simeq 4M \simeq 0.27M_e$, where M_e is the bare electronic mass. M^* increases as the square root of the magnetic field for larger magnetic fields [3]. If the density $n(\mathbf{x})$ deviates from the average density n_0 , then a residual effective magnetic field appears, equal to

$$B - 2\phi_0 n(\mathbf{x}) = 2\phi_0(n_0 - n(\mathbf{x})) = -2\phi_0 \delta n(\mathbf{x}). \quad (11)$$

3 Geometry of the experiment

The electrons are confined on a small two-dimensional ring. The ring is the set of points \mathbf{x} , such as $r_0 < |\mathbf{x}| < r_0 + L$. The dimensions of the ring are of the order $r_0 \simeq 1\mu m$ and $L \simeq 0.1\mu m$. We look for the response of the system to an extra charge Q added in the center of the ring. As we shall see in the next section, one is able to solve exactly the Schrödinger equation of the electrons on the ring in the absence of the central charge and in the absence of Coulomb interaction between electrons. The wave functions are given in terms of Bessel functions. In order to simplify the treatment of the problem, we change the geometry. (see figure 1). Instead of a ring, we shall use a rectangle of size L and $R = 2\pi r_0$. The x axis is chosen along the R side of the rectangle, and the y axis along the L side of the rectangle. We impose cyclic boundary conditions in the x direction, which means that $\psi(x + R, y) = \psi(x, y)$ for the wave functions. The spectrum and the wave functions are much more simpler for the approximate geometry. Two types of potentials in the x direction will be investigated: an infinite square well and also a parabolic well, to understand the effects of a gradual fall-off of the electronic density as may be the case in experiments.

4 $\nu = 1/2$ electrons on the ring in the absence of the central charge

One is able to solve exactly the eigenvalue problem in the absence of the central charge, in the absence of a Coulomb interaction between electrons and in the ring geometry, as well as in the simplified geometry. The magnetic field is related to the density by the condition of half filling (9), so that the total effective magnetic field through the ring is zero, and the magnetic field in the hole inside the ring is uniform and given by

$$B = 2\phi_0 n_0. \quad (12)$$

The number of electrons N on the ring is given by

$$N = \frac{\pi B L (L + 2r_0)}{2\phi_0}. \quad (13)$$

If we take $B = 20T$, the number of electrons on the ring is $N = 1494$. These N composite fermions feel a zero magnetic field, but feel the vector potential created by the flux tube in the hole of the ring. This is a typical Aharonov-Bohm situation [10] and one expects the presence of electronic currents which are periodic in φ/ϕ_0 , where φ denotes the flux in the center of the ring. Its value is simply

$$\frac{\varphi}{\phi_0} = \frac{\pi r_0^2 B}{\phi_0}. \quad (14)$$

Similar situations have already been analyzed in different geometries [11] [12]. The gauge is chosen such as $\mathbf{A}(\mathbf{x}) = A(|\mathbf{x}|)\mathbf{e}_\theta$, with

$$A(r) = \frac{\varphi}{2\pi r} \quad (15)$$

if $r > r_0$. One is left with a problem of free electrons in the vector potential $\mathbf{A}(r)$ with a Hamiltonian

$$\hat{H} = \frac{1}{2M^*}(-i\hbar\nabla + e\mathbf{A})^2. \quad (16)$$

Because of the rotational invariance of the problem, the wave functions can be chosen with a definite orbital momentum $m\hbar$

$$\psi(r, \theta) = e^{im\theta}\chi(r). \quad (17)$$

The Schrödinger equation for $\chi(r)$ reads

$$\chi''(r) + \frac{\chi(r)}{r} + (k^2 - \frac{1}{r^2}(m + \frac{\varphi}{\phi_0})^2)\chi(r) = 0, \quad (18)$$

which is a Bessel equation where we have set $E = \hbar^2 k^2 / 2M^*$. The general solution of this equation is

$$\chi(r) = AJ_{|m+\frac{\varphi}{\phi_0}|}(kr) + BY_{|m+\frac{\varphi}{\phi_0}|}(kr). \quad (19)$$

The coefficients A and B are determined by the normalisation of the wave function and by the fact that the wave function vanishes at the edges of the sample, so that $\chi(r_0) = \chi(r_0 + L) = 0$. The wave vector k is found to be the solution of

$$J_{|m+\frac{\varphi}{\phi_0}|}(kr_0)Y_{|m+\frac{\varphi}{\phi_0}|}(k(r_0 + L)) - Y_{|m+\frac{\varphi}{\phi_0}|}(kr_0)J_{|m+\frac{\varphi}{\phi_0}|}(k(r_0 + L)) = 0. \quad (20)$$

In order to obtain simpler equations for the energy levels and the wave functions, we give the form of the solution in the simplified geometry. We first treat the case $\varphi = 0$. In this case, the problem simply corresponds to free electrons on a rectangle. The wave functions are given by

$$\psi_{m,n}(x, y) = \sqrt{\frac{2}{RL}} e^{-im\frac{2\pi}{R}x} \sin\left(n\frac{\pi}{L}y\right), \quad (21)$$

and the energy levels are

$$E(m, n) = \frac{\hbar^2}{2M^*} \left(\left(\frac{2\pi}{R} \right)^2 m^2 + \left(\frac{\pi}{L} \right)^2 n^2 \right). \quad (22)$$

The electrons belong to a Fermi sea, and the Fermi wave vector k_F is approximately determined by the relation

$$k_F = \sqrt{\frac{4\pi N}{LR}}, \quad (23)$$

where the number of fermions N is given by (13). Since $L \ll R$, the wave vector increment $2\pi/R$ in the k_x direction is much smaller than the increment π/L in the k_y direction, so that the Fermi sea can be viewed as a collection of channels labeled by the integer $n > 0$. The Fermi sea is drawn on figure 2. In the case $B = 20T$, the Fermi sea is made up of six channels. In the absence of a magnetic

flux φ through the hole of the ring, or if the magnetic flux is a multiple of the flux quantum ϕ_0 , one can compute the electronic density of the Slater determinant

$$|\psi_0\rangle = \prod_{m,n \in F.S.} \psi_{m,n}^+ |0\rangle, \quad (24)$$

where the fermionic quantum numbers m and n belong to the Fermi sea of figure 2 and $|0\rangle$ is the vacuum. The density profile is plotted on figure 3. As expected, the density is zero on the edges and the density profile exhibits Friedel oscillations. The non uniformity of the density induces a non uniform electrostatic field, which modifies the one-particle states. Thus, due to finite size effects, (24) is not the true ground state for the mean field approximation, whereas it would be the true ground state on an infinite plane.

What happens if the flux φ in the hole of the ring is non zero? Let us first consider the case where φ/ϕ_0 is an integer. As we see from equation (18), we can deduce the physics from the case $\varphi = 0$ by replacing m by $m + \varphi/\phi_0$. The Fermi sea is translated in the reciprocal space by a factor $\Delta k_x = 2\pi\varphi/R\phi_0$ along the k_x direction.

If φ/ϕ_0 is not an integer, the situation is somewhat different. One expects in this case the appearance of a current due to an Aharonov-Bohm effect [13]. We note $\varphi/\phi_0 = \Delta m + \delta m$, with Δm an integer and δm a real number, such as $|\delta m| < 1/2$. The energy $E(m, n)$ reads

$$E(m, n) = \frac{\hbar^2}{2M^*} \left[\left(\frac{2\pi}{R} \right)^2 (m + \Delta m + \delta m)^2 + \left(\frac{\pi}{L} \right)^2 n^2 \right]. \quad (25)$$

The Fermi sea is translated by the wave vector $\Delta k_x = -2\pi\Delta m/R$, so that the wave functions become

$$\psi_{m,n}(x, y) = \sqrt{\frac{2}{RL}} e^{i(m-\Delta m)\frac{2\pi}{R}x} \sin n\frac{\pi}{L}y \quad (26)$$

The Fermi sea becomes unstable as $|m| = 1/2$. To see this, consider $2N_0 + 1$ fermions in a given channel n . If $|\delta m|$ is less than $1/2$, the fermions have the possibility to have their orbital quantum numbers in the interval $[-\Delta m - N_0, -\Delta m + N_0]$, or in the interval $[-\Delta m - N_0 \pm 1, -\Delta m + N_0 \pm 1]$. The condition for the latter configuration to be stable is that it has a lower energy than the former, namely

$$\frac{\hbar^2}{2M^*} \left(\frac{2\pi}{R} \right)^2 \sum_{m=-\Delta m-N_0}^{-\Delta m+N_0} (m + \Delta m + \delta m)^2 < \frac{\hbar^2}{2M^*} \left(\frac{2\pi}{R} \right)^2 \sum_{m=-\Delta m-N_0 \pm 1}^{-\Delta m+N_0 \pm 1} (m + \Delta m + \delta m)^2, \quad (27)$$

which is satisfied for $|\delta m| < 1/2$, independently on N_0 . The Fermi sea of $2N_0 + 1$ fermions in the channel n is thus in the interval $m \in [\Delta m - N_0, \Delta m + N_0]$ if $-1/2 < \delta m < 1/2$. What is the Aharonov-Bohm current in the ring for a non integer value of φ/ϕ_0 ? The quantum mechanical, gauge invariant current operator reads

$$\mathbf{j}(\mathbf{x}) = \frac{-i\hbar}{2M^*} (\bar{\psi} \nabla \psi - \psi \nabla \bar{\psi}) + \frac{e}{M^*} \mathbf{A} |\psi|^2. \quad (28)$$

In the simplified geometry, the current has only a component parallel to the x axis. The contribution of the first term in (28) is

$$\frac{\hbar}{M^*} \frac{2\pi}{R} (m - \Delta m), \quad (29)$$

and the contribution of the term proportional to the vector potential reads

$$\frac{\hbar}{M^*} \frac{2\pi}{R} (\Delta m + \delta m). \quad (30)$$

The total current is thus

$$j_x(m, n) = \frac{\hbar}{M^*} \frac{2\pi}{R} (m + \delta m) |\psi_{m,n}|^2. \quad (31)$$

After a summation over the Fermi sea, we obtain the total current

$$J_x(y) = \sum_{(m,n) \in F.S.} j_x(m, n) = \frac{2\hbar}{M^*} \frac{2\pi}{R} \delta m \sum_{(m,n) \in F.S.} |\psi_{m,n}|^2, \quad (32)$$

If $\delta m = 0$, the flux in the hole of the ring is a multiple of the flux quantum, and everything happens as if the fermions would not see the flux. If $\delta m \neq 0$, a current exists. The intensity of the current is given by

$$I = -e \int_0^L J_x(y) dy = -\frac{2\pi e \hbar N}{M^* R^2} \delta m. \quad (33)$$

The maximum value of the current is

$$I_{max} = \frac{e \hbar N}{2 M^* R^2}. \quad (34)$$

The numerical value of I_{max} is $5.8 nA$ for $B = 20T$.

5 $\nu = 1/2$ electrons on a ring in the presence of the external charge

In the presence of a positive central charge, the electrons are expected to accumulate near the internal edge of the ring and a depletion of electrons is expected at the external edge, leading to a charge transfer from the external to the internal edge. This charge transfer induces a deviation from the $\nu = 1/2$ value and, if one applies the ideas of the mean field theory, the total effective flux, due to the external magnetic field plus the statistical gauge field is no longer zero, so that an effective flux penetrates through the sample, creating an Aharonov-Bohm current which is periodic as a function of the central charge.

The first step is to evaluate the screening of the central charge by the electron gas on the ring. Many levels of approximation are possible. The most accurate approximation is to take into account that the one particle Slater determinant (24) is not the true ground state of the fermions, due to Friedel oscillations induced by the edges. This can be implemented in a recursive way by starting from the state (24), computing the electronic density, deducing from it the electrostatic field, and reiterating, that is to compute the corrections to the one-particle states in the presence of the Friedel

oscillations, and re-compute the electronic density. The effect of the charge is then treated at the linear order, with the full response function. Within these approximations, one expects the density of electrons to increase near the internal edge of the ring, and to decrease near the external edge. Moreover, this average density profile should be modulated by Friedel oscillations as well as oscillations at the Thomas-Fermi wave vector. In our case, as we shall see, the Thomas-Fermi wave vector is greater than the Fermi wave vector. We shall not use this refined approximation scheme because of its computational complexity. Since we focus only on the charge transfer from one edge of the ring to the other, and not on the details of the variations of the density profile, we do not take into account the existence of Friedel oscillations. We take the state (24) as an approximate ground state and we look for the effects of the screening of the central charge. In other words, we hope the density-density response functions are not very different if we replace the true Hartree-Fock state by the approximate one given by (24).

At this stage, two approximations are possible. The most refined one consists in taking into account the full response function of the fermions. This shall be done in section 5.4. A more approximate treatment is to treat the screening in the Thomas-Fermi approximation, which is the aim of section 5.3. As we shall see, the two approximations lead to similar results as far as averaged quantities are concerned, namely the average effective flux penetrating through the ring due to the presence of the central charge.

5.1 Screening in two dimensions

As an introduction to the problem of screening in a finite geometry, we treat the case of the screening of a single charge in an infinite two-dimensional gas of electrons. The solution of this problem will lead to the expression of the Thomas-Fermi wave vector q_{TF} in two dimensions. The case of the screening of a charge in three dimensions is treated in reference [14] with the Thomas-Fermi approximation. We do nothing but transpose the argument of [14] to the case of an electron gas constrained on a two-dimensional layer, with three dimensional Coulomb interactions. The potential created by the external point charge located at the origin is noted ϕ^{ext} . We note ρ^{ind} the variation of density induced by the presence of the extra charge in the gas of electrons, plus the uniform background of positive charges. ϕ is the total potential created by the extra charge, the electrons and the background of positive charges. Since the two-dimensional Fourier transform of $1/|\mathbf{x}|$ is $2\pi/|\mathbf{q}|$, we have

$$\phi(\mathbf{q}) - \phi^{ext}(\mathbf{q}) = \frac{\rho^{ind}(\mathbf{q})}{2\epsilon_0\epsilon_r|\mathbf{q}|}. \quad (35)$$

The dielectric constant is defined by $\phi^{ext}(\mathbf{q}) = \epsilon(\mathbf{q})\phi(\mathbf{q})$, and we assume that $\rho^{ind}(\mathbf{q}) = \chi(\mathbf{q})\phi(\mathbf{q})$. We thus obtain

$$\epsilon(\mathbf{q}) = 1 - \frac{\chi(\mathbf{q})}{2\epsilon_0\epsilon_r|\mathbf{q}|}. \quad (36)$$

If the total potential is a slowly varying function of the position, one can define

$$\epsilon(\mathbf{k}) = \frac{\hbar^2 \mathbf{k}^2}{2M^*} - e\phi(\mathbf{x}), \quad (37)$$

so that the local distribution function reads

$$n(\mathbf{x}) = \int \frac{d\mathbf{k}}{(2\pi)^2} \frac{1}{1 + \exp\{\beta(\hbar^2 \mathbf{k}^2 / 2M^* - e\phi(\mathbf{x}) - \mu)\}}, \quad (38)$$

and the density of the background positive charge is

$$n^0(\mu) = \int \frac{d\mathbf{k}}{(2\pi)^2} \frac{1}{1 + \exp\{\beta(\hbar^2 \mathbf{k}^2 / 2M^* - \mu)\}}. \quad (39)$$

Thus, we can write the induced density of electrons as $\rho^{ind}(\mathbf{x}) = -e\{n^0(\mu + e\phi(\mathbf{x})) - n^0(\mu)\}$. If ϕ is small, $\rho^{ind}(\mathbf{x}) = -e^2 \partial n^0 / \partial \mu \phi(\mathbf{x})$, so that

$$\chi(\mathbf{q}) = -e^2 \frac{\partial n^0}{\partial \mu} = -\frac{M^* e^2}{2\pi \hbar^2}. \quad (40)$$

The dielectric constant reads $\epsilon(\mathbf{q}) = 1 + q_{TF}/|\mathbf{q}|$, where q_{TF} is the Thomas-Fermi wave vector

$$q_{TF} = \frac{M^*}{\hbar^2} \frac{e^2}{4\pi\epsilon_0\epsilon_r}. \quad (41)$$

If one adds an extra charge Q at the origin,

$$\phi(\mathbf{q}) = \frac{1}{\epsilon(\mathbf{q})} \phi^{ext}(\mathbf{q}) = \frac{Q}{2\epsilon_0} \frac{1}{|\mathbf{q}| + q_{TF}}. \quad (42)$$

A Fourier transform yields

$$\phi(\mathbf{x}) = \frac{Q}{4\pi\epsilon_0|\mathbf{x}|} F(q_{TF}|\mathbf{x}|), \quad (43)$$

with

$$F(z) = \int_0^{+\infty} J_0(u) \frac{u}{u+z} du. \quad (44)$$

The interaction is screened if $x \gg 2\pi/q_{TF}$. The numerical value of the Thomas-Fermi length $\lambda_{TF} = 2\pi/q_{TF}$ is $\lambda_{TF} = 15.6\text{nm}$.

5.2 Linear response approach

The aim of the section is to present the real space linear response formalism. From a numerical point of view, this means that we must discretize the radial coordinate at a scale smaller than the Thomas-Fermi length λ_{TF} . Within the linear response, the density variation is linearly related to the local potential, but in a non local way:

$$\delta\rho(\mathbf{x}) = \int_0^L \chi^{(0)}(x, x') V_{loc}(x') dx', \quad (45)$$

where $x \in [0, L]$ is the radial coordinate, with the origin taken at the interior edge of the ring. Notice that the conservation of charge carriers implies that

$$\int_0^L \chi^{(0)}(x, x') dx = 0. \quad (46)$$

The local potential is the sum of the potential created by the electrostatic field of the central charge $V_{ext}(x)$, plus the potential $V_{ind}(x)$ induced by the electrons on the ring. Since the distance L between the two edges is small ($L = 0.1 \mu m$), we linearize the Coulomb potential created by the central charge in the vicinity of the ring, which leads to the following expression of $V_{ext}(x)$:

$$V_{ext}(x) = \frac{Qe^2}{4\pi\epsilon_0\epsilon_r(r_0 + L/2)^2} \left(x - \frac{L}{2}\right) \quad (47)$$

On the other hand, the induced potential has the expression

$$V_{ind}(x) = \frac{e^2}{4\pi\epsilon_0\epsilon_r} \int_0^L \left(1 + \frac{x'}{r_0}\right) \delta\rho(x') dx' \quad (48)$$

$$\int_{-\pi}^{\pi} \frac{d\theta}{\sqrt{(1 + \frac{x}{r_0})^2 + (1 + \frac{x'}{r_0})^2 - 2(1 + \frac{x}{r_0})(1 + \frac{x'}{r_0}) \cos \theta}}. \quad (49)$$

Using the notations $u = 1 + x/r_0$ and $v = 1 + x'/r_0$, the angular integral takes the form of an elliptic integral

$$\int_{-\pi}^{\pi} \frac{d\theta}{\sqrt{u^2 + v^2 - 2uv \cos \theta}} = 4 \int_0^{\pi/2} \frac{d\theta}{\sqrt{(u+v)^2 - 4uv \cos^2 \theta}} = \frac{4}{u+v} K\left(\frac{2\sqrt{uv}}{u+v}\right). \quad (50)$$

Since u and v are close to unity, the elliptic integral can be approximated as

$$K\left(\frac{2\sqrt{uv}}{u+v}\right) = \ln\left(\frac{4|u+v|}{|u-v|}\right) + O\left((u-v)^2 \ln|u-v|\right), \quad (51)$$

which leads to

$$V_{ind}(x) \simeq \frac{e^2}{2\pi\epsilon_0\epsilon_r} \int_0^L \ln\left(\frac{8r_0}{|x-x'|}\right) \delta\rho(x') dx' \quad (52)$$

Notice that the factor $8r_0$ does not come into account since

$$\int_0^L \delta\rho(x) dx = 0. \quad (53)$$

The equation (45) reads

$$\delta\rho = \chi^{(0)}(V_{ext} + V_{ind}\delta\rho), \quad (54)$$

where the quantities are understood as matrices for $\chi^{(0)}$ and V_{ind} and vectors for $\delta\rho$ and V_{loc} . A discretization of the radial coordinate has been assumed, and we used a parabolic approximation for the integrals. A special attention has to be paid to the logarithmic divergence of (52) which has to be integrated explicitly using a parabolic approximation. Equation (54) can be inverted into the form

$$\delta\rho = \frac{1}{1 - \chi^{(0)}V_{ind}} \chi^{(0)}V_{ext}, \quad (55)$$

which has the well known form of a R.P.A. resummation. Numerically, we use a Gauss-Jordan method for inverting the linear system (52). The size of the matrix to be inverted is about 1000, which corresponds to 1000 points for the discretization of the interval $[0, L]$. Since $L \sim 0.1\mu m$, the condition $L/1000 \ll \lambda_{TF}$ is well respected. We now examine successively two levels of approximation for the response function $\chi^{(0)}(x, x')$.

5.3 Thomas-Fermi approach to the response function

In the Thomas-Fermi approach, the response function is purely local:

$$\chi_{TF}^{(0)}(x, x') = -\frac{m}{2\pi\hbar^2}(\delta(x - x') - \frac{1}{a}) \quad (56)$$

Using this form of the response function, we inverted the system (54). The resulting density profile is given on figure 4. In terms of the effective flux through the sample (flux of the magnetic field plus flux of the statistical gauge field), one is interested in

$$\phi(x) = -4\pi\phi_0(r_0 + L/2) \int_0^x \delta\rho(x)dx. \quad (57)$$

The function $\phi(x)$ is plotted on figure 5. As we shall see in section 5.5, the total current is given in terms of the mean flux through the ring

$$\bar{\phi} = \frac{1}{L} \int_0^L \phi(x)dx \quad (58)$$

We find that $\bar{\phi}$ is such that a charge $Q = 14e^-$ is required to induce one flux quantum on average through the ring, which means that the periodicity of the currents as a function of the central charge is 14 electrons within the infinite square well potential and the Thomas Fermi approximation.

5.4 Screening of the central charge with the full response function

We calculate the full response function using the first order perturbation theory in the potential induced by the central charge. We also use the simplified geometry. The matrix elements of the local potential V_{loc} on the basis of function (21) are

$$V_{n,n'}^{loc} = \frac{2}{L} \int_0^L \sin\left(\frac{\pi}{L}nx\right) V_{loc}(x) \sin\left(\frac{\pi}{L}n'x\right) dx, \quad (59)$$

so that

$$\hat{V}_{loc} = \sum_m \sum_{n,n'} V_{n,n'}^{loc} \psi_{m,n}^+ \psi_{m,n'}. \quad (60)$$

The first order corrections to the state $|\psi_0\rangle$ of equation (24) are

$$|\psi\rangle = |\psi_0\rangle + \sum_m \sum_{n,n'} \frac{V_{n,n'}^{loc}}{E(m, n') - E(m, n)} \psi_{m,n}^+ \psi_{m,n'} |\psi_0\rangle. \quad (61)$$

The second-quantized form of the electron density operator is

$$\hat{\rho}(x, y) = \frac{2}{RL} \sum_{m, m'} \sum_{n, n'} e^{-i(m' - m)\frac{2\pi}{R}x} \sin\left(\frac{\pi}{L}ny\right) \sin\left(\frac{\pi}{L}n'y\right) \psi_{m, n}^+ \psi_{m', n'} |\psi_0\rangle. \quad (62)$$

One can readily calculate the average of $\hat{\rho}(x, y)$ in the presence of the central charge, which leads to

$$\begin{aligned} \langle \hat{\rho}(x, y) \rangle_Q - \langle \hat{\rho}(x, y) \rangle_{Q=0} &= \frac{4}{RL} \sum_m \sum_{n, n'} \frac{V_{n, n'}}{E(m, n') - E(m, n)} n^0(m, n') \\ &\quad (1 - n^0(m, n)) \sin\left(\frac{\pi}{L}ny\right) \sin\left(\frac{\pi}{L}n'y\right), \end{aligned} \quad (63)$$

where $n^0(n, m)$ is unity if (m, n) belongs to the Fermi sea and zero otherwise. The summation over m can be evaluated by noticing that the Fermi sea is made up of a collection of nested one dimensional Fermi seas (one for each channel), and we obtain

$$\begin{aligned} \delta \langle \hat{\rho}(x, y) \rangle &= \frac{8M^*}{\pi^2 \hbar^2} \left\{ \sum_{n=1}^N \sum_{n'=n+1}^N \frac{\sqrt{\nu^2 - n^2} - \sqrt{\nu^2 - n'^2}}{n^2 - n'^2} \sin\left(\frac{\pi}{L}ny\right) \sin\left(\frac{\pi}{L}n'y\right) V_{n, n'}^{loc} \right. \\ &\quad \left. + \sum_{n=1}^N \sum_{n'=N+1}^{+\infty} \frac{\sqrt{\nu^2 - n^2}}{n^2 - n'^2} \sin\left(\frac{\pi}{L}ny\right) \sin\left(\frac{\pi}{L}n'y\right) V_{n, n'}^{loc} \right\}. \end{aligned} \quad (64)$$

In this expression, ν is related to the Fermi energy by

$$E_F = \frac{\hbar^2}{2M^*} \frac{\pi^2}{L^2} \nu^2 \quad (65)$$

and N is the integer such as $\nu \in [N, N+1[$. We deduce from (64) the response function $\chi^{(0)}(y, y')$:

$$\chi^{(0)} = \frac{16M^*}{\pi^2 \hbar^2 L} \left\{ \sum_{n=1}^N \sum_{n'=n+1}^N \frac{\sqrt{\nu^2 - n^2} - \sqrt{\nu^2 - n'^2}}{n^2 - n'^2} \Lambda_{n, n'}^{(ISW)}(y, y') + \sum_{n=1}^N \sum_{n'=N+1}^{+\infty} \frac{\sqrt{\nu^2 - n^2}}{n^2 - n'^2} \Lambda_{n, n'}^{(ISW)}(y, y') \right\}, \quad (66)$$

with

$$\Lambda_{n, n'}^{(ISW)}(y, y') = \sin\left(\frac{\pi}{L}ny\right) \sin\left(\frac{\pi}{L}n'y\right) \sin\left(\frac{\pi}{L}ny'\right) \sin\left(\frac{\pi}{L}n'y'\right). \quad (67)$$

The symbol IFW stands for "infinite square well". With the form (66) for $\chi^{(0)}$, it is straightforward to compute the density of electrons, using the matrix relation (55). The profile of the electron density variations induced by the central charge is plotted on figure 6. We notice the existence of oscillations at the Thomas-Fermi wave vector, which were absent in the calculation using the Thomas-Fermi approach to the response function. However, these oscillations do not affect too much the averaged quantities under interest. The total flux through the sample $\phi(x)$ is plotted on figure 7, and has the same shape as the flux computed in the Thomas-Fermi approximation. The mean flux through the ring is such as 18.2 e^- are required to produce one flux quantum through the ring within the infinite square well approximation and within a calculation including the full response function.

5.5 Electrons in a parabolic potential well

In experiments, the edges of the ring may not be so well-defined, and the electronic density will exhibit a gradual fall off to zero. This section is devoted to model the effects of ill-defined edges. To do so, we use the same techniques as before, and use a parabolic confining well instead of an infinitely deep well. Within the mean field treatment, the Hamiltonian of the quasiparticles reads

$$H = \frac{\hat{p}^2}{2M^*} + \frac{1}{2}M^*\omega^2 y^2. \quad (68)$$

As before, we start from a Slater determinant (24), with one electron wave functions

$$\varphi_{m,n}(x, y) = \frac{1}{\sqrt{R}} \left(\frac{\beta^2}{\pi} \right)^{1/4} \frac{1}{\sqrt{2^n n!}} \exp \left(-\frac{\beta^2 y^2}{2} \right) H_n(\beta y) e^{-im \frac{2\pi}{R} x} \quad (69)$$

where the inverse length scale β is

$$\beta = \sqrt{\frac{M^* \omega}{\hbar}} \quad (70)$$

and H_n are the Hermite polynomials. The radial density of the Slater determinant is plotted on figure 8, where the strength of the harmonic potential has been adjusted such as 70% of the electronic density lies within the one micrometer wide ring. Friedel oscillations are visible. From a computational point of view, the Hermite polynomials may reach huge values. It is thus more practical to calculate recursively $\tilde{H}_n = H_n/\sqrt{2^n n!}$, with the following recursion relations

$$\tilde{H}_{n+1}(u) = \sqrt{\frac{2}{n+1}} u \tilde{H}_n(u) - \sqrt{\frac{n}{n+1}} \tilde{H}_{n-1}(u), \quad (71)$$

and $\tilde{H}_0(u) = 1$, $\tilde{H}_1(u) = \sqrt{2}u$. The same approach as in section 5.4 can be carried out and the response function is

$$\chi^{(0)} = \frac{2\sqrt{2}}{\pi^2} \frac{M^* \beta}{\hbar^2} e^{-\beta(y^2 + y'^2)} \left\{ \sum_{n=0}^N \sum_{n'=n+1}^N \frac{\sqrt{\nu-n} - \sqrt{\nu-n'}}{n-n'} \Lambda_{n,n'}^{(HW)}(y, y') + \sum_{n=0}^N \sum_{n'=N+1}^{+\infty} \frac{\sqrt{\nu-n}}{n-n'} \Lambda_{n,n'}^{(HW)}(y, y') \right\}, \quad (72)$$

with

$$\Lambda_{n,n'}(y, y') = \tilde{H}_n(\beta y) \tilde{H}_{n'}(\beta y) \tilde{H}_n(\beta y') \tilde{H}_{n'}(\beta y'), \quad (73)$$

and ν is defined by $E_F = (\nu + 1/2)\hbar\omega$. Using similar techniques as in section 5.4, we get the radial density variations (figure 9) as well as the induced flux (figure 10). We come to the conclusion that a central charge approximately equal to 9 electrons is required to generate one flux quantum through the ring, which suggests that the Fermi sea in a parabolic well is more sensitive to the central charge as in the infinite square well. This is due to the fact that the fraction of the electronic density outside the $0.1\mu m$ ring experience is closer to the central charge (as far as the inner edge is concerned) and thus experiences a stronger potential. We conclude to the importance of whether there is a sharp edge or a graduate fall-off to zero of the electronic density. In the former case, one flux quantum could be generated through the ring with a smaller charge than in the latter case.

5.6 Currents induced by the charge

The magnetic flux through the ring generates permanent currents, in the same way as a flux through the hole of the ring generates currents. Let us call $\delta\mathbf{A}$ the variation in the vector potential due to the presence of the charge. The variation in the Hamiltonian due to the shift in the vector potential is

$$\delta H = \frac{e^2}{2M^*}(2\mathbf{A} \cdot \delta\mathbf{A} + \delta\mathbf{A}^2) + \frac{ie\hbar}{M}\delta\mathbf{A} \cdot \nabla. \quad (74)$$

Applying first order perturbation theory, we obtain the variation of a given energy level

$$\langle\delta H\rangle = \frac{e^2}{M^*}\langle\mathbf{A} \cdot \delta\mathbf{A}\rangle - \frac{e\hbar}{M^*}m\langle\frac{\delta A(r)}{r}\rangle. \quad (75)$$

We now make the approximation that the spatial dependence of $\delta\mathbf{A}$ and $\delta A(r)/r$ are averaged on the ring, that is to say

$$\frac{\delta A(r)}{r} \simeq \frac{\overline{\phi}}{2\pi r_0^2}, \quad (76)$$

where $\overline{\phi}$ is the average magnetic flux induced by the central electric charge. The first term in δH is simply an energy variation independent on n and m . This term is then dropped. Thus we get

$$\langle\delta H\rangle = -\frac{e\hbar}{M^*}m\frac{\overline{\phi}}{2\pi r_0^2}, \quad (77)$$

so that the total energy reads

$$E(m, n) = \frac{\hbar^2}{2M^*r_0^2}(m - \frac{\overline{\phi}}{\phi_0})^2 - \frac{\hbar^2}{2Mr_0^2}(\frac{\overline{\phi}}{\phi_0})^2. \quad (78)$$

If we apply the result of section 4 about Aharonov Bohm currents, we find that the currents are periodic in $\overline{\phi}$. The maximum value of the current is given by (34) and the period is such as $\overline{\phi} = \phi_0$.

6 Numerical approach in the spherical geometry

We now make use of the spherical geometry in order to perform numerical computations with a small number of electrons on a sphere of radius R . A magnetic monopole is put at the center of the sphere, creating a total magnetic flux through the sphere equal to $2S\phi_0$. The Dirac's monopole quantization requires $2S$ to be an integer. An electric charge Q is put at the north pole of the sphere. The extra charge is treated as a classical, point charge. We first generalize the mean field theory argument to the spherical geometry case. In a second step, we present numerical computations for a small number of electrons on the sphere for various filling fractions.

6.1 Mean field theory at $\nu = 1/2$

We adapt the argument of the mean field theory, previously established in the geometry of the ring, to the spherical geometry. The filling fraction

$$\nu = \frac{N-1}{2S} \quad (79)$$

is chosen to be $1/2$ in this section. The non local gauge transformation leads to a statistical field which generates a flux equal to $-2\phi_0(N-1)$ because there is no statistical flux coming from a particle onto itself. The mean field Hamiltonian simply corresponds to fermions on the sphere in the absence of a magnetic field. If one neglects the Coulomb interactions, the Hamiltonian is diagonal on the basis of the spherical harmonics $Y_{l,m}(\theta, \varphi)$ normalized such as

$$\int Y_{l,m}(\theta, \varphi) d\Omega = 1 \quad (80)$$

The wave function is simply $\psi_{l,m}(\theta, \varphi) = Y_{l,m}(\theta, \varphi)/R$. The single particle states are labelled by the positive integer l and the integer m such as $-l \leq m \leq l$. The energy of a state labelled by (l, m) reads

$$E(l, m) = \frac{\hbar^2}{2M^*R^2} l(l+1). \quad (81)$$

In the presence of a negative (positive) electric charge at the north pole, a depletion (accumulation) of electrons arises at the north pole, and an accumulation (depletion) arises at the south pole. The mean field model in the presence of the charge at the north pole consists of electrons in a zero magnetic field plus a flux tube $\bar{\phi}$ penetrating through the south pole and emerging at the north pole. The problem of quantum motion around a flux tube $\bar{\phi} = \alpha\phi_0$ in the spherical geometry was considered in [16]. We now rederive the solution. This problem is non perturbative in $\bar{\phi}$, since infinite quantities appear in the first order perturbation theory in $\bar{\phi}$. This is why we adopt an algebraic approach. The flux tube $\bar{\phi}$ is absorbed in a gauge transformation, leading to multivalued wave functions

$$\psi(r, \theta + 2\pi) = e^{2i\pi\gamma} \psi(r, \theta). \quad (82)$$

The eigenvalues of l_z are thus quantized by $l_z = m + 2\pi\gamma$, m being an integer. The eigenstates of the Hamiltonian are also eigenstates of \mathbf{l}^2 , since

$$H = -\frac{\hbar^2}{2m} \Delta = -\frac{\hbar^2}{2M^*R^2} \mathbf{l}^2. \quad (83)$$

A priori, it is not obvious to produce a basis of common eigenvectors to \mathbf{l}^2 and l_z , since the rotational invariance is broken by the presence of the flux tube. Nonetheless, as we shall see, it is possible to diagonalize simultaneously \mathbf{l}^2 and l_z . The spherical representation of the kinetic momentum algebra is [17]:

$$l^+ = e^{i\varphi} \left(\frac{\partial}{\partial \theta} + i \cot \theta \frac{\partial}{\partial \varphi} \right) \quad (84)$$

$$l^- = e^{-i\varphi} \left(-\frac{\partial}{\partial\theta} + i \cot\theta \frac{\partial}{\partial\varphi} \right) \quad (85)$$

$$l_z = \frac{1}{2}[l^+, l^-] = \frac{1}{i} \frac{\partial}{\partial\varphi} \quad (86)$$

The operator algebra gives rise to two ladders of states. The $(-)$ ladder corresponds to states descending, by the repeated action of l^- , from the highest weight state $\psi_0^{(-)}$, such as $l^+ \psi_0^{(-)} = 0$. The states $\psi_0^{(-)}$ have the form

$$\psi_0^{(-)}(\theta, \varphi) = f^{(-)}(\theta) e^{i(l+\gamma)\varphi}, \quad (87)$$

with l an integer, and is such as

$$\left(\frac{\partial}{\partial\theta} + i \cot\theta \frac{\partial}{\partial\varphi} \right) e^{i(l+\gamma)\varphi} f^{(-)}(\theta) = 0, \quad (88)$$

so that $f^{(-)}(\theta) \propto (\sin\theta)^{l+\gamma}$, with $l+\gamma > 0$. We take $\gamma \in]0, 1[$, and $l = 0, 1, \dots$. For a given l , we can produce $l+1$ descending states by the repeated action of l^- . For these states, $l_z = \gamma, 1+\gamma, \dots, l+\gamma$ and $l^2 = (l+\gamma)(l+\gamma+1)$. The $(+)$ ladder correspond to states ascending, by the repeated action of l^+ , from the highest weight state $\psi_0^{(+)}$ such as $l^- \psi_0^{(+)} = 0$. $\psi_0^{(+)}$ has the form

$$\psi_0^{(+)}(\theta, \varphi) = f^{(+)}(\theta) e^{i(l+\gamma)\varphi}, \quad (89)$$

with l an integer, and is such as

$$\left(-\frac{\partial}{\partial\theta} + i \cot\theta \frac{\partial}{\partial\varphi} \right) e^{i(l+\gamma)\varphi} f^{(+)}(\theta) = 0, \quad (90)$$

so that $f^{(+)}(\theta) \propto (\sin\theta)^{-(l+\gamma)}$, with $l+\gamma < 0$, so that $|l| \leq -1$. The repeated action of l^+ produces $|l|$ states with $l_z = l+\gamma, l+\gamma+1, \dots, -1+\gamma$ and $l^2 = (l+\gamma)(l-1+\gamma)$.

We now enumerate the first states. With $l = 0$, $E = \gamma(\gamma+1)$ and the degeneracy g is 1. With $l = -1$, $E = (1-\gamma)(2-\gamma)$ and $g = 1$. With $l = 1$, $E = (1+\gamma)(2+\gamma)$ and $g = 2$. If $l = -2$, $E = (2-\gamma)(3-\gamma)$ and $g = 2$. If $l = 2$, $E = (2+\gamma)(3+\gamma)$ and $g = 3$. If $l = -p$, $E = (p-\gamma)(p+1-\gamma)$ and $g = p$ and if $l = p$, $E = (p+\gamma)(p+1+\gamma)$ and $g = p+1$.

We now turn to the calculation of permanent currents, since this is the quantity we shall compute using numerical diagonalizations for a small number of electrons. We distinguish between two cases: $p(p-1) \leq N \leq p^2$ and $p^2 \leq N \leq p(p+1)$. First, if $p(p-1) \leq N \leq p^2$, we note $\lambda = N - p(p-1)$. The total energy is given by

$$E_{tot} = \sum_{m=1}^{p-1} ((m-1+|\gamma|)(m+|\gamma|) + (m-|\gamma|)(m+1-|\gamma|)) m + (p-1+|\gamma|)(p+|\gamma|) \lambda \quad (91)$$

$$= \frac{1}{2} p^2 (p-1)^2 + p(p-1) \lambda + ((2p-1)\lambda - p(p-1)) |\gamma| + (\lambda + p(p-1)) \gamma^2 \quad (92)$$

for $\gamma \in [-1/2, 1/2]$. If $p^2 \leq N \leq p(p+1)$, we note $\lambda' = N - p^2$ and, for $\gamma \in [-1/2, 1/2]$, we obtain

$$E_{tot} = \frac{1}{2} p^2 (p-1)^2 + p^2 (p-1) + p(p+1) \lambda' + (p^2 - (2p+1) \lambda') |\gamma| + (p^2 + \lambda') \gamma^2. \quad (93)$$

The current $dE_{tot}/d\gamma$ is discontinuous for half integer values of γ , as for the ring, but further discontinuities appear for integer values of γ . The jump in the current at $\gamma = 0$ is

$$\frac{dE_{tot}}{d\gamma}(0^+) - \frac{dE_{tot}}{d\gamma}(0^-) = 2((2p-1)\lambda - p(p-1)), \quad (94)$$

or

$$\frac{dE_{tot}}{d\gamma}(0^+) - \frac{dE_{tot}}{d\gamma}(0^-) = 2(p^2 - (2p+1)\lambda'). \quad (95)$$

The first term corresponds to the case $p(p-1) \leq N \leq p^2$, and the second case to $p^2 \leq N \leq p(p+1)$. The jump of the current at $\gamma = 1/2$ is

$$\frac{dE_{tot}}{d\gamma}(\frac{1}{2}^+) - \frac{dE_{tot}}{d\gamma}(\frac{1}{2}^-) = -4p\lambda, \quad (96)$$

or

$$\frac{dE_{tot}}{d\gamma}(\frac{1}{2}^+) - \frac{dE_{tot}}{d\gamma}(\frac{1}{2}^-) = -4p(p - \lambda'). \quad (97)$$

6.2 Numerical procedure

We assume that the magnetic field is large enough to neglect the excitations from the first Landau level to higher Landau levels. We propose to diagonalize numerically the Coulomb interaction inside the Hilbert space generated by the set of the occupations of the lowest Landau level. The quantum Hall effect on the sphere has been studied by Haldane [15]. He proposes a set of coherent states which span the lowest Landau level Hilbert space. From this set of coherent states, we can extract the following basis of the lowest Landau level Hilbert space

$$\phi_\alpha(\mathbf{x}) = \langle \mathbf{x} | \alpha \rangle = N_\alpha (\sin \frac{\theta}{2})^\alpha (\cos \frac{\theta}{2})^{2S-\alpha} e^{i\varphi(S-\alpha)}, \quad (98)$$

where N_α is chosen in such a way that

$$\int |\phi_\alpha(\mathbf{x})|^2 d\mathbf{x} = 1. \quad (99)$$

The label α indexes the orbitals of the lowest Landau level and runs from 0 to $2S$. One needs to compute the matrix elements of the Coulomb interaction. The interaction V_1 between the electrons on the sphere and the classical charge located at the north pole is a one-body operator and the interactions V_2 between the electrons on the sphere is represented by a two-body operator. Using the second quantization, it is straightforward to derive expressions for the matrix elements of \hat{V}_1 and \hat{V}_2 on the basis of the states with all the possible occupation numbers of the lowest Landau level. We do not give here the details of the calculations. We used the the results of [20] relating the matrix elements of the Coulomb potential to Clebsch–Gordan coefficients. One is left with a symmetric matrix to be diagonalized using a Lanczos method in each sector of the z component of the angular momentum (since the Hamiltonian is invariant under any rotation around the z axis). The ground state is used to calculate the expectation value of the one-body current operator. The total intensity is obtained after an integration of the current $j(\theta)$ over the angular coordinate θ .

6.3 Results

We diagonalized the Coulomb interaction at half filling with $N = 8$ electrons (figure 12) and $N = 9$ electrons (figure 13). Obviously, the intensity is not periodic as the central charge varies. This is due to the fact that only a small number of electrons is present in our numerical diagonalizations. As the central charge is tuned, level crossing occurs, namely the z component of the angular momentum of the ground state is varied as the central charge is varied. Notice that these level crossings are allowed because they correspond to crossing of levels in different sectors of the Hilbert space. Due to the small number of electrons, as the central classical charge is increased, one reaches a point where no more crossing occurs since the Hilbert space, restricted to the lowest Landau level is finite. Above this point, the intensity saturates. If the central charge is large and positive, the electrons are attracted at the north pole and the current is thus positive. By contrast, if the classical charge is large and negative, the electrons are repelled from the north pole, and mainly located on the south hemisphere, and the current is negative (see figure 14). However, if the classical charge is not too important, we observe discontinuous variations of the intensity as a function of the central charge, which is very much reminiscent of the previously calculated mean field behavior even though we were not able to related the position of the discontinuities to the ones of the mean field model. We checked that the discontinuities in the current correspond to level crossings at the bottom of the spectrum in the sense that each jump in the current is associated with the fact that the z component of the angular momentum of the ground state changes. We conclude that the mean field scenario for the intensity as a function of the central charge is qualitatively supported by our numerical calculations. At the quantitative level, it seems rather difficult to conclude since we can only carry out numerical diagonalizations for a small number of electrons. In particular, we cannot conclude on the existence of periodic variations of the intensity as a function of the classical charge since the available sizes are too small.

7 Conclusion

We have shown that a charge in the middle of ring of $\nu = 1/2$ electrons induces currents which vary periodically as a function of the central charge. The mechanism for the generation of these periodic currents involves a polarization of the electron liquid on the ring. If the extra charge is positive, a positive density variation appears on the interior edge of the ring, and a depletion of negative charges appears on the external edge of the sample. These charges screen the field of the central charge. The appearance of currents on the ring is mediated by the variation of the Chern-Simons gauge field at mean field level. The presence of polarization charges on the edges on the sample induces a non-zero average flux through the ring. By increasing the charge, one should be able to produce periodic currents in the ring. The order of magnitude of these Aharonov-Bohm currents is such that they can be measured [19]. The amplitude of the current fluctuations is typically 2.0 nA

for a ring of radius $1\ \mu m$ and transverse dimension $0.1\ \mu m$ and a magnetic field of 20 T. If one can produce a continuous charge in the middle of the ring, one should be able to find experimentally the period of the phenomenon. Our mean field calculations show that the period is of the order of 14 electrons (calculated with the full response function) with an infinite square potential. However, the periodicity of the phenomenon is sensitive to the existence of a graduate density fall-off at the edges, as is expected to occur in experiments. In the case of a parabolic well with 30% of the electronic density outside the 0.1 micrometer ring, we found a 9 electrons periodicity. Residual currents should also appear in the absence of the charge, because of the presence of a magnetic flux through the ring. The experimental observation of such currents should be a direct test of the existence of a statistical gauge field in the $\nu = 1/2$ quantum Hall effect. We also carried out numerical computations in the spherical geometry. The mean field picture at $\nu = 1/2$ predicts discontinuities in the intensity plotted as a function of the extra charge and also the existence of periodic variations. In our simulations, the current is not periodic as a function of the charge at the north pole, because of a too small number of electrons. However, we find the existence of discontinuities, reminiscent of the predictions of the mean field treatment. We conclude to the qualitative consistency between our numerical diagonalizations and the mean field theory.

Our analysis shows that the type of experiment we consider would be a good test for the mean field theory of the $\nu = 1/2$ quantum Hall effect since the presence of an extra charge allows to explore excited states properties, and this in a way which goes beyond linear response theory, since it involves level crossings and non-trivial reshuffling of the many body ground state as the external charge is varied.

Finally, the case $\nu = 1/3$ would also be an interesting case to examine and the physics might be quite different from the $\nu = 1/2$ case investigated here. It would be especially interesting to understand the interplay between incompressible bulk excitations and compressible edge states [21] as the central charge is varied. This question will be addressed in a future work.

The authors acknowledge L. Lévy for stimulating discussions which encouraged us to carry on this investigation. R.M. acknowledges J.C. Anglès d'Auriac and F.V. de Abreu for assistance with the numerical work.

References

- [1] J.K. Jain, Phys. Rev. Lett. 63, 199 (1989); Phys. Rev. B 41, 7653 (1990); Adv. Phys. 41, 105 (1992).
- [2] R.L. Willet et al, Phys. Rev. Lett. 71, 3846 (1993); W Kang et al, Phys. Rev. Lett. 71, 3850 (1993); R.R. Du et al, Phys. Rev. Lett. 70, 2944 (1993); D.R. Leadley et al, Phys. Rev. Lett. 72, 1906 (1994); R.R. Du et al, Solid State Comm. 90, 71 (1994); V.J. Goldman, B. Su and J.K. Jain, Phys. Rev. Lett. 72, 2065 (1994).
- [3] B.I. Halperin, P.A. Lee and N. Read, Phys. Rev. B 47, 7312 (1993); see also A. Lopez and E. Fradkin, Phys. Rev. B 44, 5246 (1991); V. Kalmeyer and S.C. Zhang, Phys. Rev. B 46, 9889 (1992).
- [4] Y.B. Kim, P.A. Lee, X.G. Wen and P.C.E. Stamp, Phys. Rev. B 51, 10779 (1995); A. Stern and B.I. Halperin, Harvard University preprint (1995).
- [5] Compare for instance the paper by D.R. Leadley et al and the second paper by R.R. Du et al in Ref. [2].
- [6] E. Rezzayi and N. Read, Phys. Rev. Lett. 72, 900 (1994).
- [7] R. Morf and N. d'Ambrumenil, Phys. Rev. Lett. 74, 5116 (1995).
- [8] Y. Aharonov and A. Casher, Phys. Rev. Lett. 53, 319 (1984).
- [9] W.J. Elion, J.J. Wachters, L.L. Sohn and J.E. Mooij, Phys. Rev. Lett. 71, 2311 (1993).
- [10] Y. Aharanov, D. Bohm, Phys. Rev. 115, 125 (1959).
- [11] E.N. Bogachek, G.A. Gogadze, J.E.T.P. 36, 973 (1973).
- [12] M.S. Svirskii, J.E.T.P. Lett. 42, 270 (1985).
- [13] See for instance M. Büttiker, Y. Imry and R. Landauer, Phys. Lett. 96 A, 365 (1983).
- [14] N.W. Ashcroft and N.D. Mermin *Solid State Physics*, Saunders (1976).
- [15] F.D.M. Haldane, Phys. Rev. Lett. 51, 605 (1983).
- [16] S. Olariu and I. Popescu, Rev. Mod. Phys. 57, 339 (1985).
- [17] R. Shankar *Principles of Quantum Mechanics*, Plenum Press, New York (1980) pp 343-345.
- [18] S.H. Simon and B.I. Halperin, Phys. Rev. B 50, 1807 (1994) and S. He, S.H. Simon and B.I. Halperin, Ibid, 50, 1823 (1994).

- [19] D. Mailly, C. Chapelier and A. Benoît, Phys. Rev. Lett. 70, 2020 (1993).
- [20] G. Fano, F. Ortolani and E. Colombo, Phys. Rev. B 34, 2670 (1986).
- [21] X.G. Wen, Phys. Rev. B 41, 12838 (1990); X.G. Wen, Phys. Rev. Lett. 64, 2206 (1990); E.H. Rezayi and F.D.M. Haldane, Phys. Rev. B 50, 17199 (1994).

Figure captions

Figure 1:

(a): annulus geometry. (b): simplified geometry.

Figure 2:

Fermi sea of quasiparticles at the mean field level in the simplified geometry. k_x is a multiple of $2\pi/R$ and k_y is a multiple of π/L .

Figure 3:

Electronic density of the Slater determinant (24) $\rho(x) = |\langle x|\psi_0\rangle|^2$. The electronic density vanishes at the edges and exhibits Friedel oscillations. The fermi sea contains 6 channels and 1494 electrons. The density is plotted in μm^{-2} and the radial coordinate in μm . The electrons are confined in an infinite square well.

Figure 4:

Profile of the electronic density variations induced by the central charge in the Thomas-Fermi approach to the response function. The computation has been made in the simplified geometry. The central charge is $Q = -1e^-$. The density is plotted in μm^{-2} and the radial coordinate in μm . The electrons are confined in an infinite square well.

Figure 5:

Flux through the ring in the Thomas-Fermi approach to the response function. The central charge is $Q = -1e^-$. The flux is plotted in units of the flux quantum ϕ_0 and the radial coordinate in μm . The electrons are confined in an infinite square well.

Figure 6:

Profile of the electronic density variations induced by the central charge with the full response function. The computation has been made in the simplified geometry. The central charge is $Q = -1e^-$. The density is plotted in μm^{-2} and the radial coordinate in μm . The electrons are confined in an infinite square well.

Figure 7:

Flux through the ring with the full response function. The central charge is $Q = -1e^-$. The flux is plotted in units of the flux quantum ϕ_0 and the radial coordinate in μm . The origin of the radial coordinate is chosen at the inner edge. The unit length is the micrometer and the density is measured in micrometers⁻². The electrons are confined in an infinite square well.

Figure 8:

Radial density of the Slater determinant with a parabolic potential well. The Fermi sea contains 8 channels and the strength of the parabolic potential has been adjusted such as 70% of the density is located on the 1 micrometer wide ring. Friedel oscillations are visible. The radial coordinate is counted in micrometers from the inner edge. The density is measured in micrometers⁻².

Figure 9:

Variations of the electronic density induced by a central charge equal to minus one electron, with a parabolic confining potential. The origin of distances is the center of the ring (minimum of the potential). The distances are measured in micrometers and the density in micrometers⁻².

Figure 10:

Flux through the ring induced by a central charge equals to minus one electron with a parabolic confining well. The distances are measured in micrometers and the densities are in micrometers⁻². The origin of the radial coordinate is the center of the well.

Figure 11:

Variations of the electronic current as a function of the central charge in the mean field approach. The period of the variations depends of the type of approximation (Thomas Fermi or full response function) and on the nature of the confining well (see the text). The residual current at $Q = 0$ originates from the Aharonov-Bohm currents induced by the presence of the flux in the hole of the ring.

Figure 12:

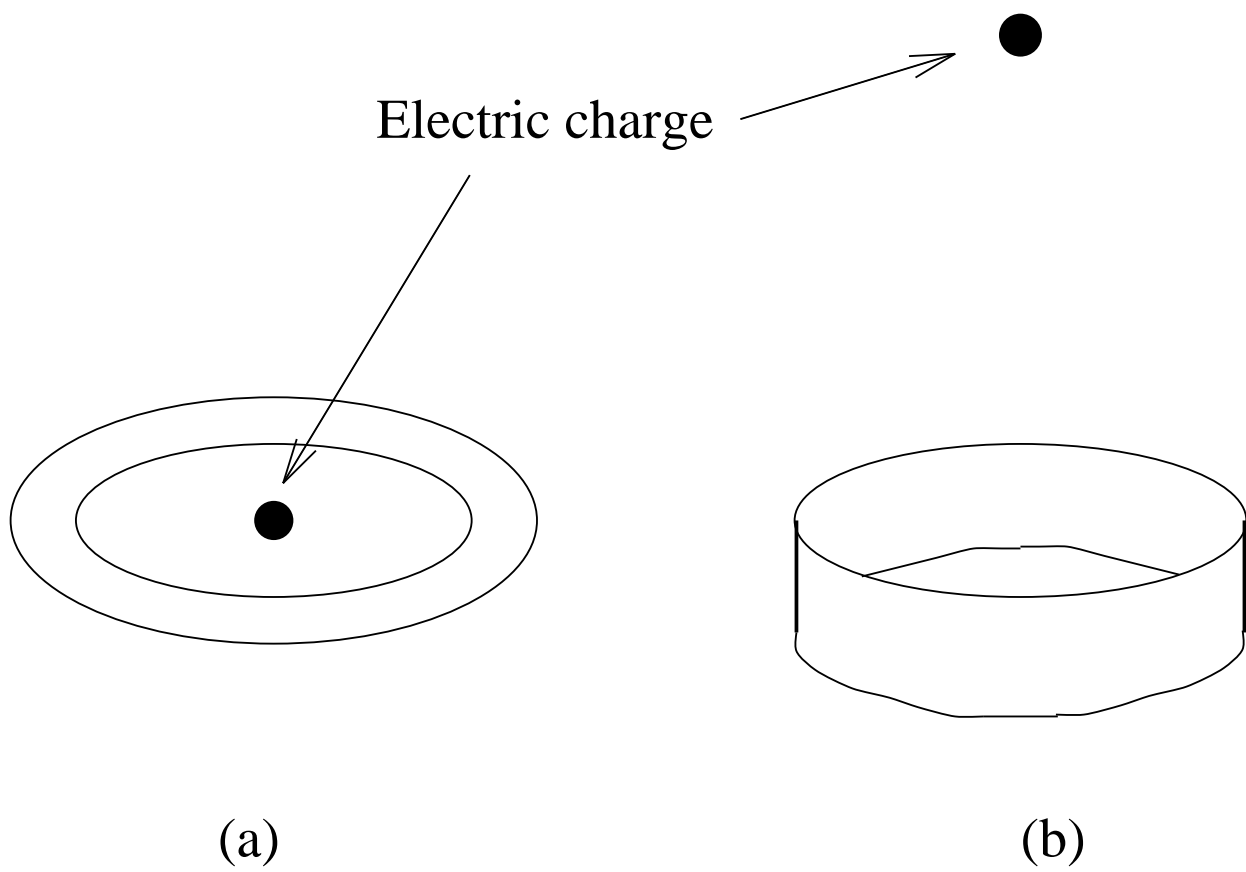
Current as a function of the classical charge located at the north pole. The intensity is $I = \int j(\theta)d\theta$. The radius R of the sphere is taken to be 1. The charge $-Q$ is plotted in units of the electronic charge e . The current is plotted in units of $2e\hbar/M^*$. The system contains 8 electrons.

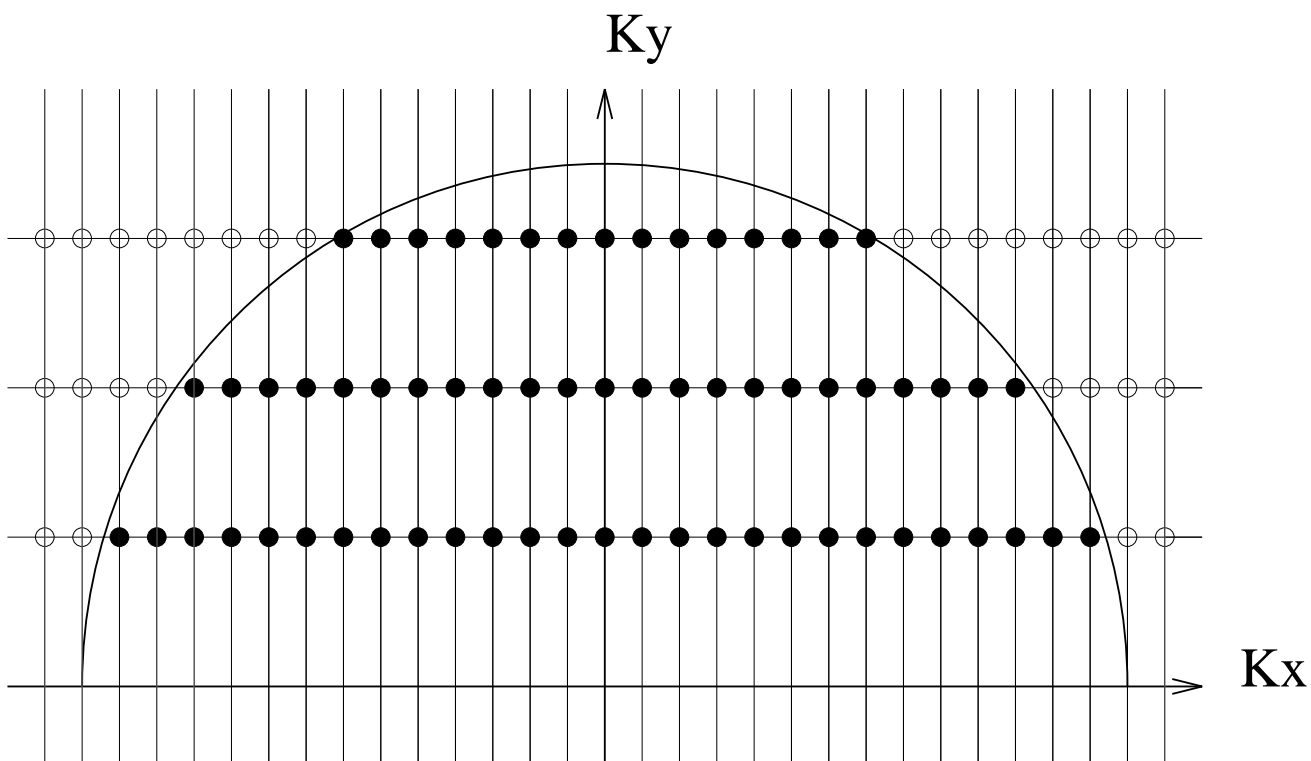
Figure 13:

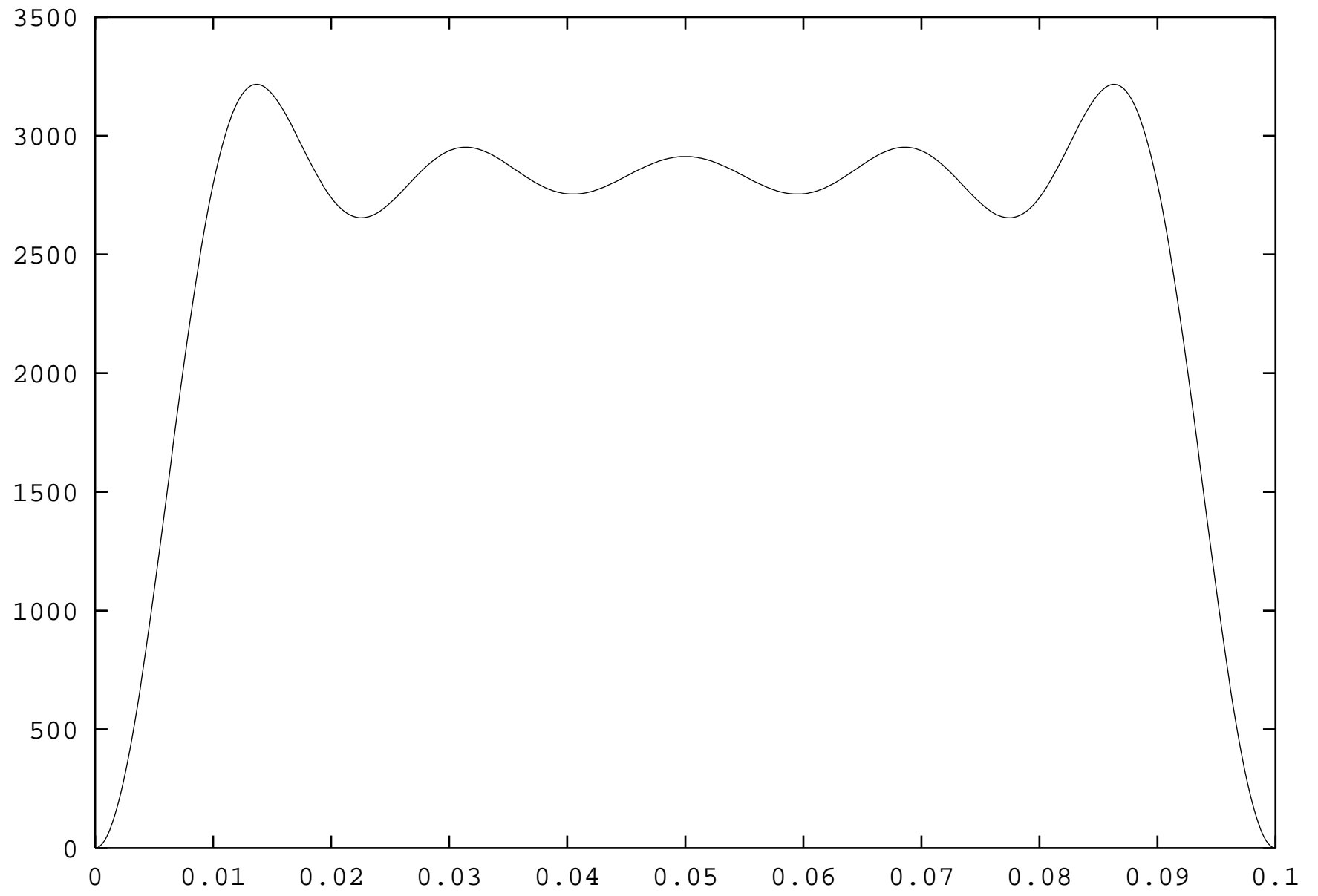
Current as a function of the classical charge located at the north pole. The intensity is $I = \int j(\theta)d\theta$. The radius R of the sphere is taken to be 1. The charge $-Q$ is plotted in units of the electronic charge e . The current is plotted in units of $2e\hbar/M^*$. The system contains 9 electrons.

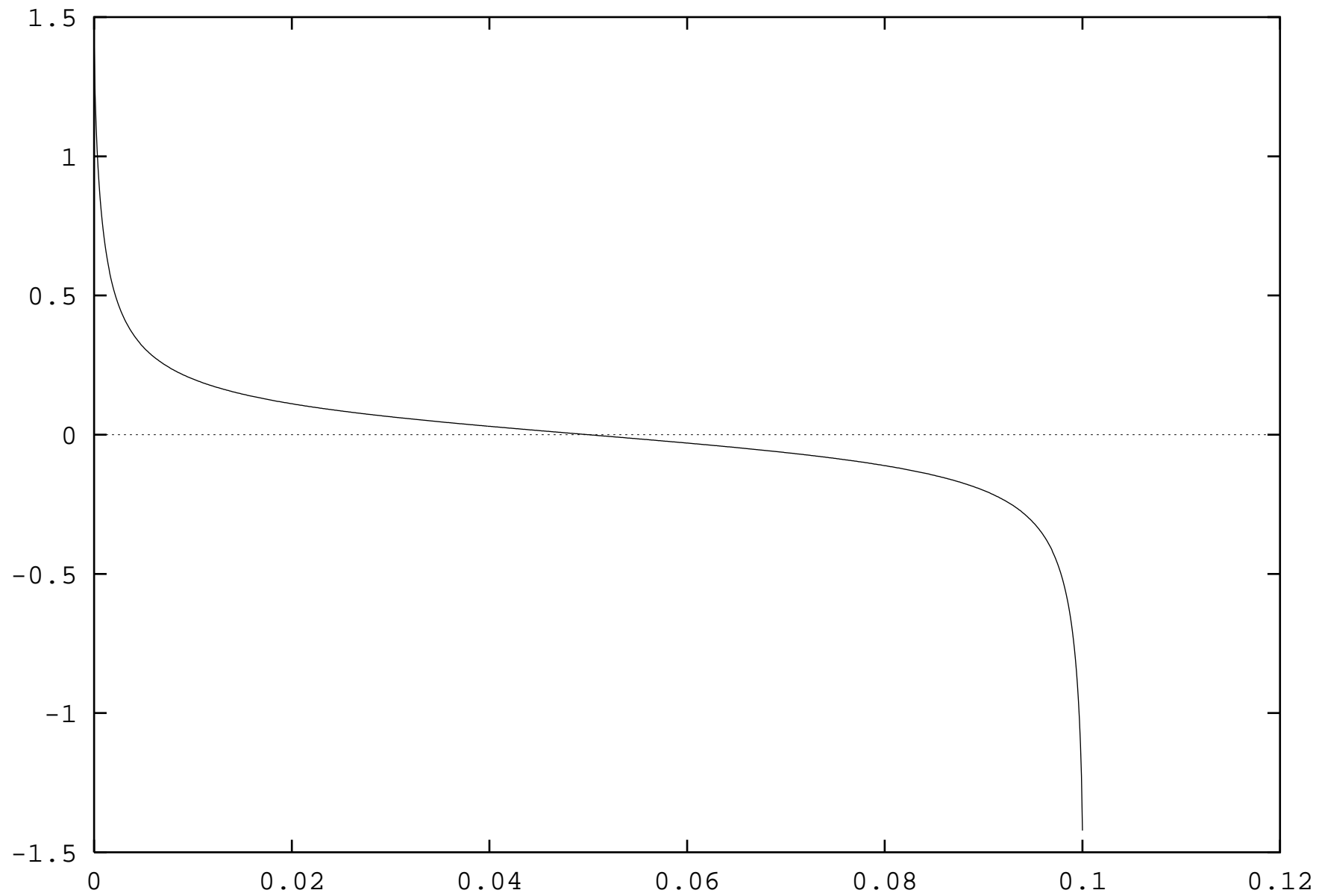
Figure 14:

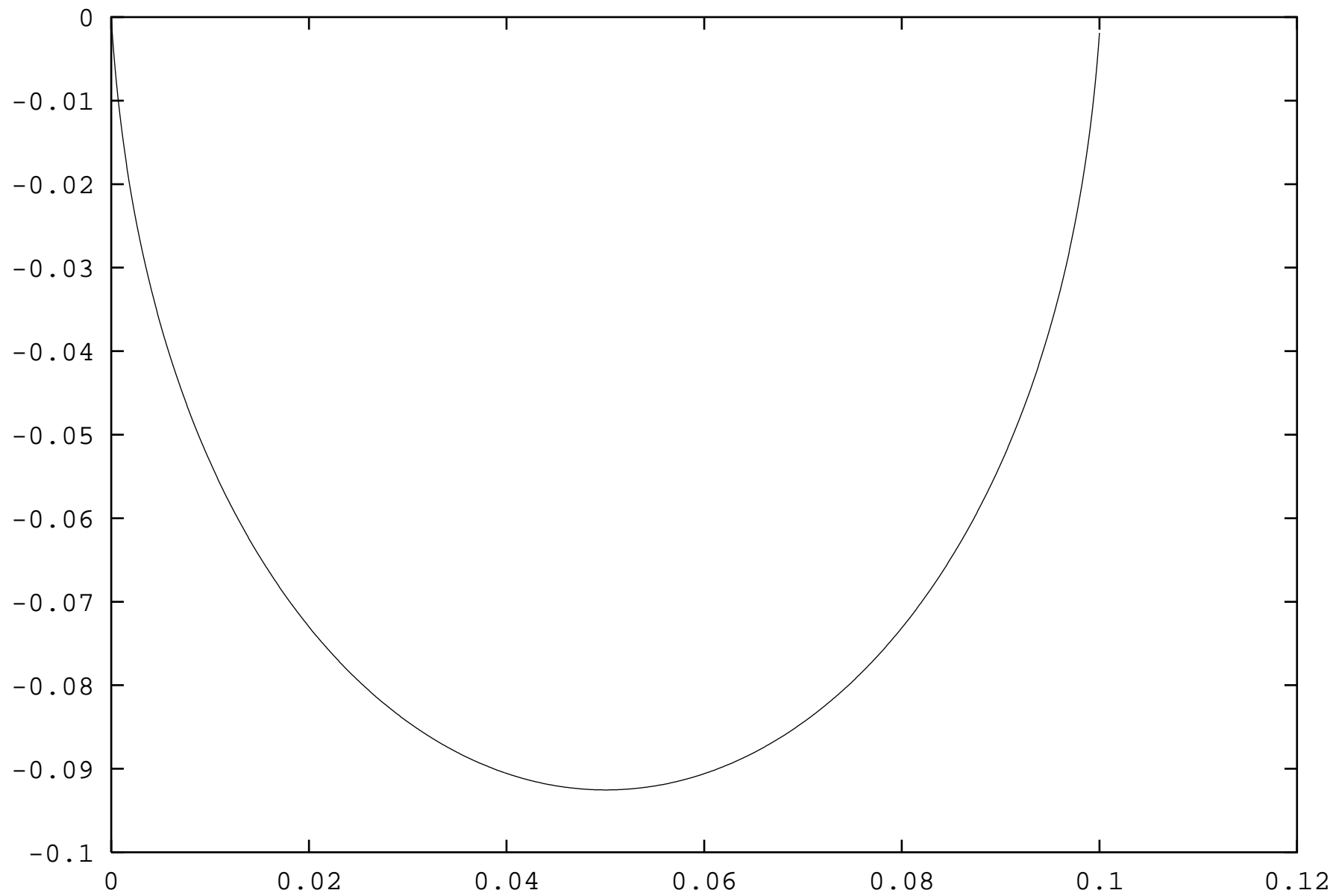
Current circulation on the sphere for a large positive classical charge (a) and a large negative classical charge (b). In (a) the electrons gather at the north pole, due to the attractive Coulomb interaction between the electron gas and the classical charge. The current in this case is clockwise. In (b), the electrons are repelled from the north pole and the circulation of the current is counterclockwise.



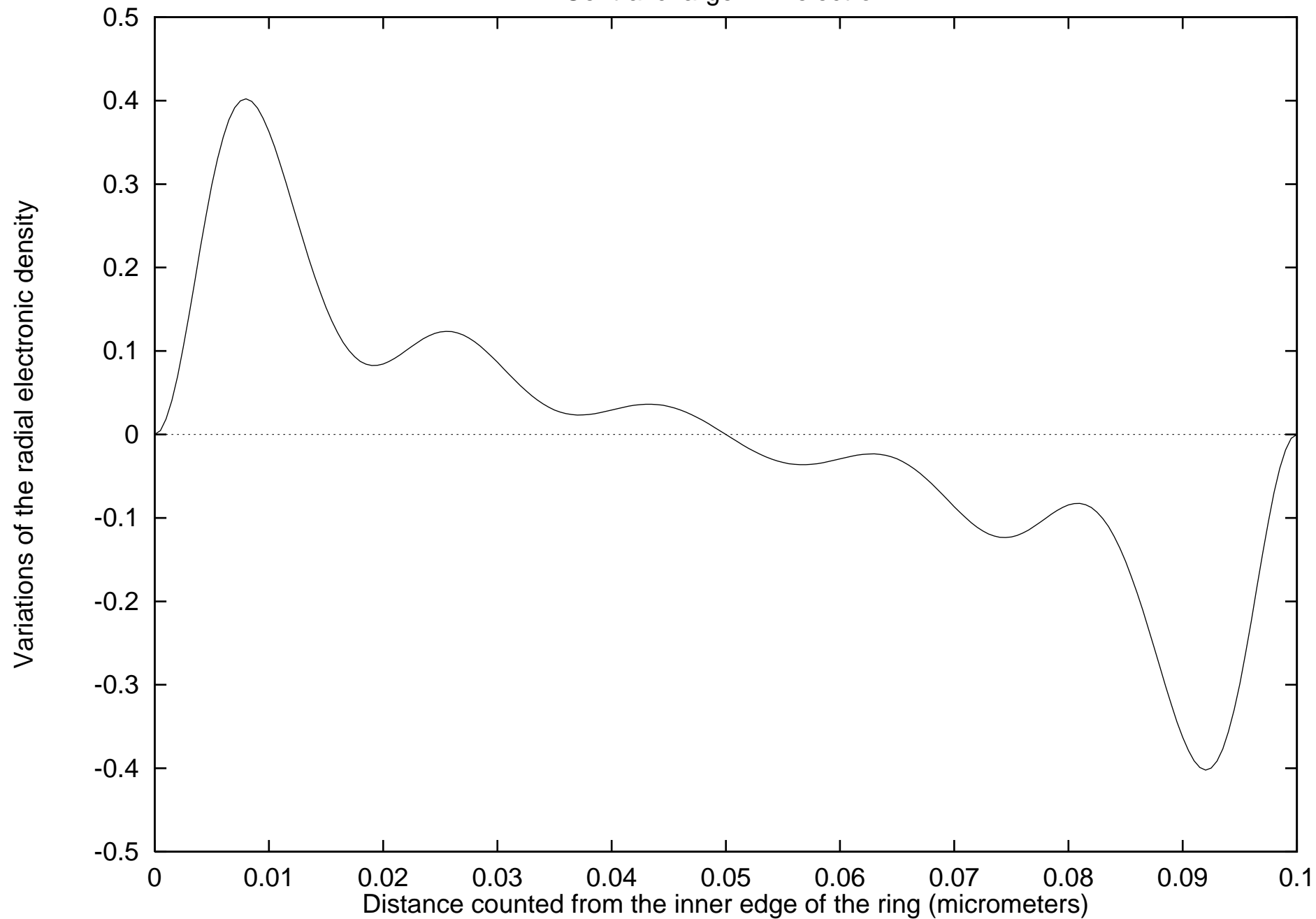




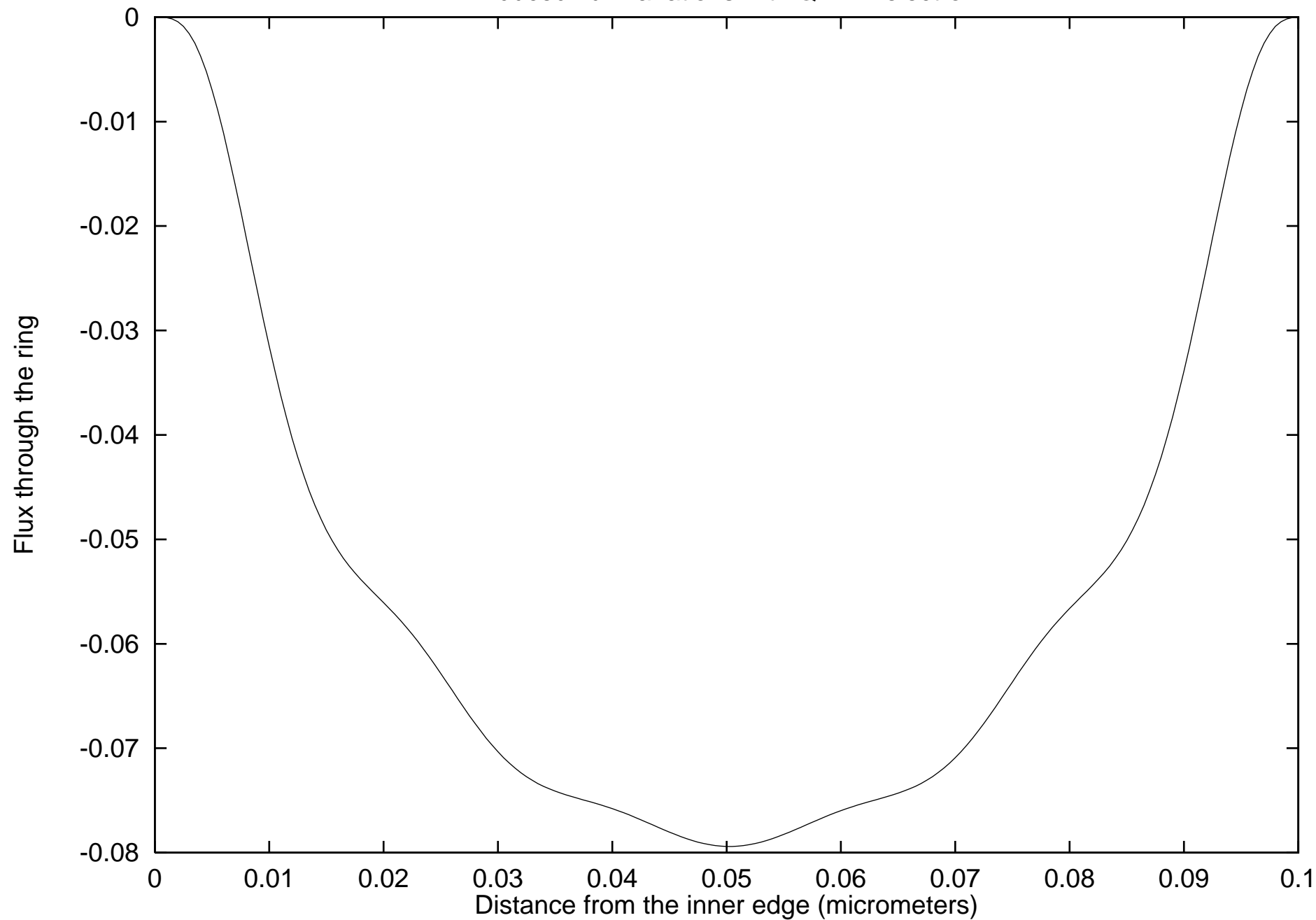




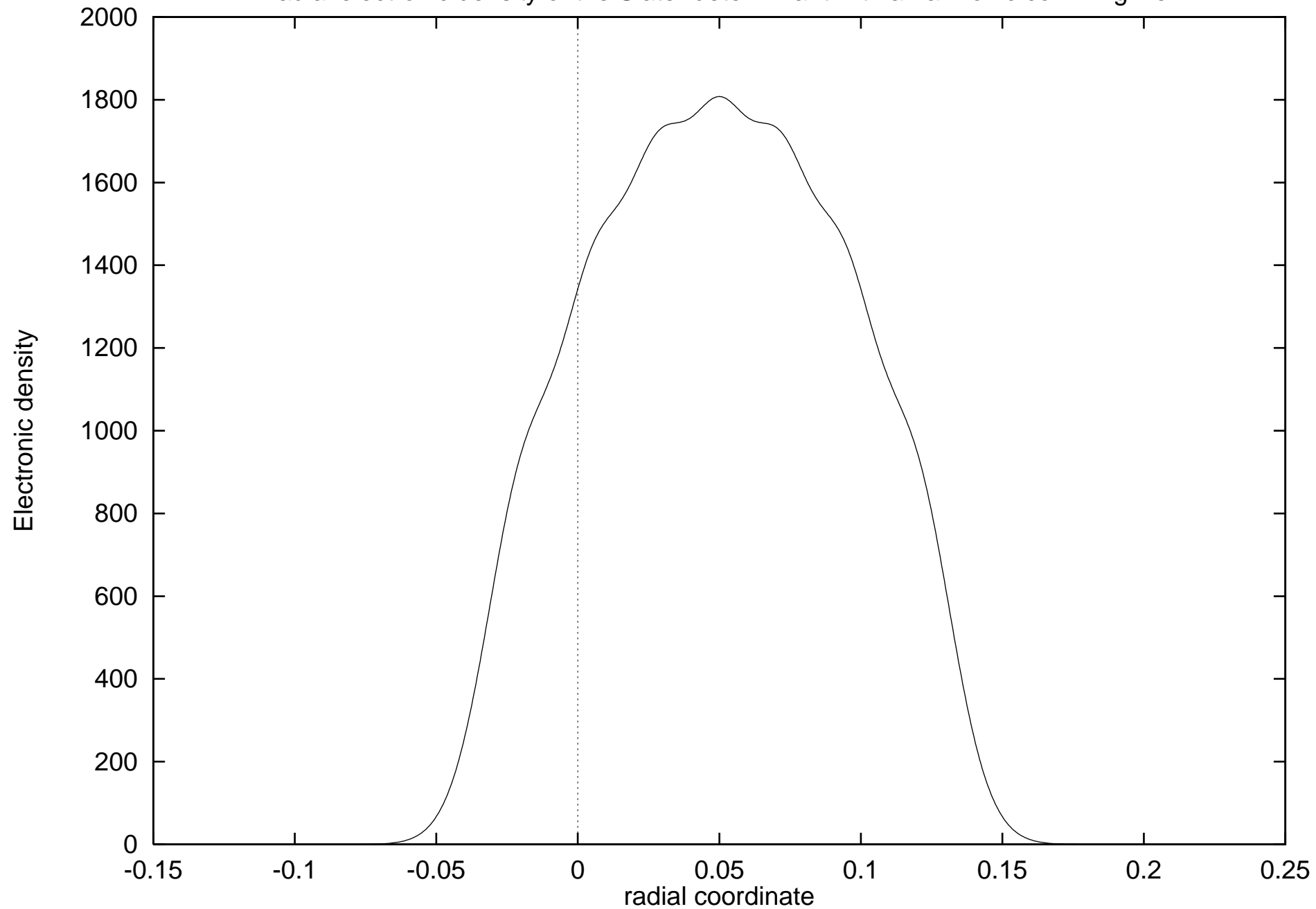
Central charge = -1 electron



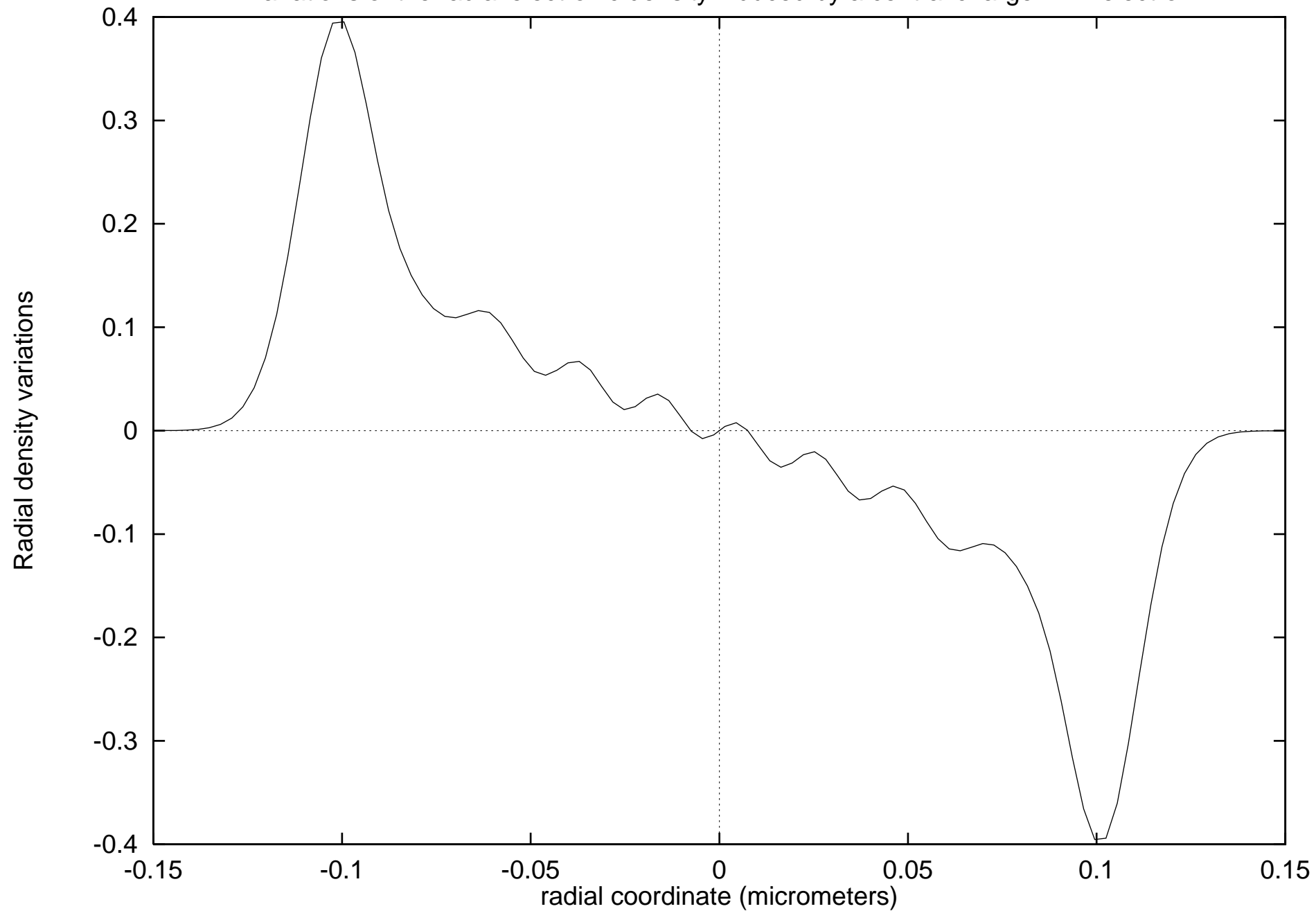
Induced flux variations with $Q = -1$ electron



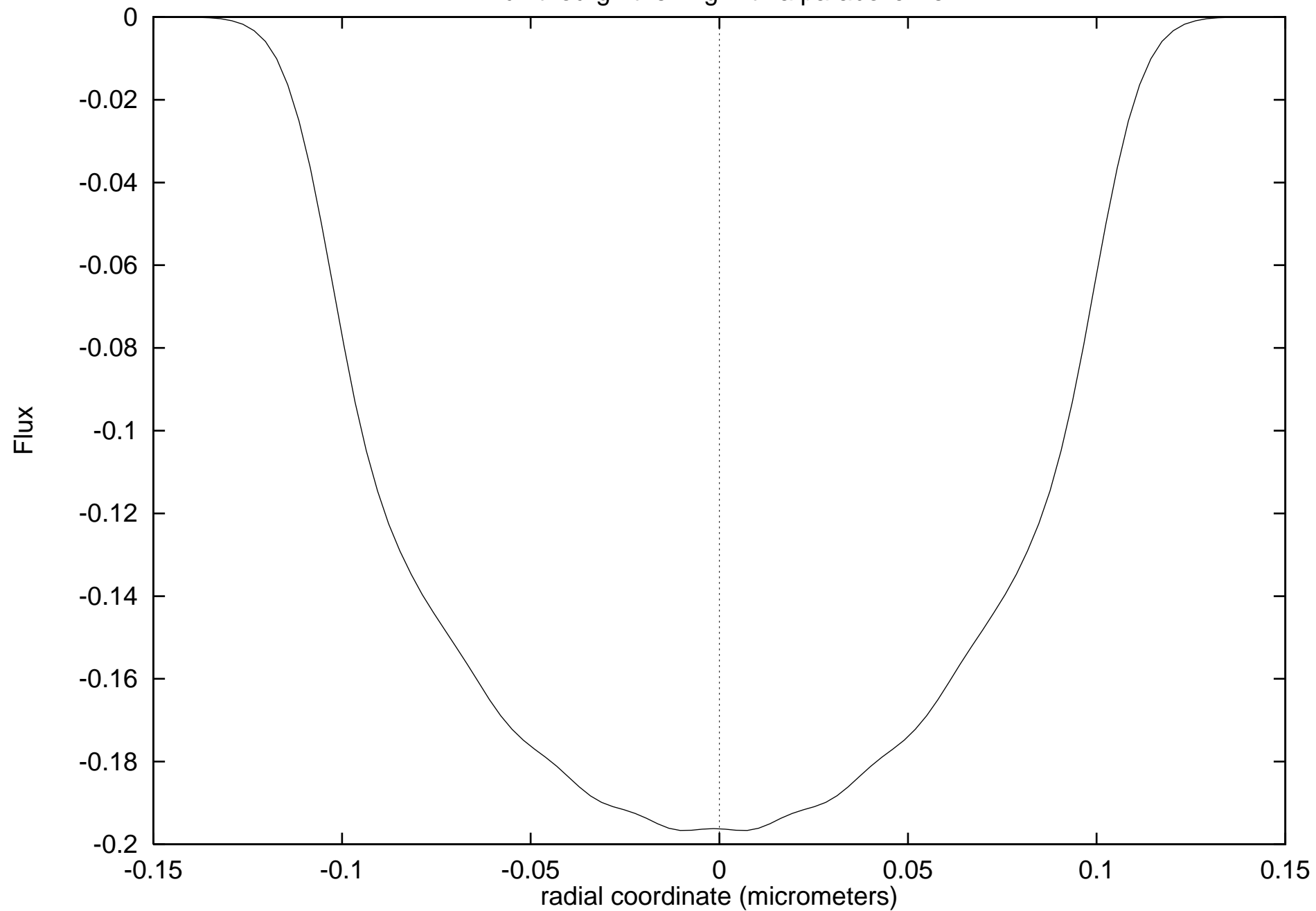
Radial electronic density of the Slater determinant with a harmonic confining well

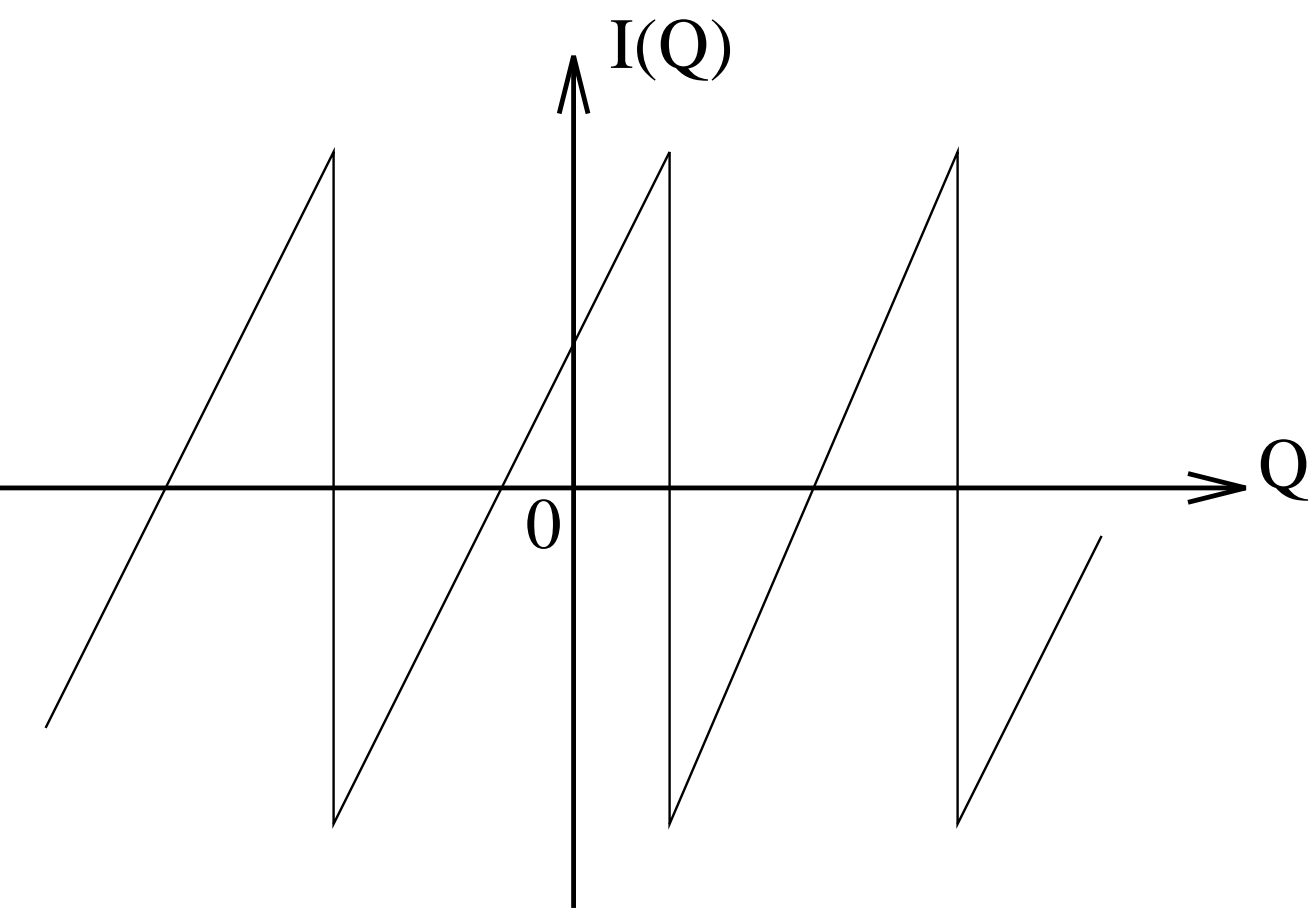


Variations of the radial electronic density induced by a central charge = - 1 electron

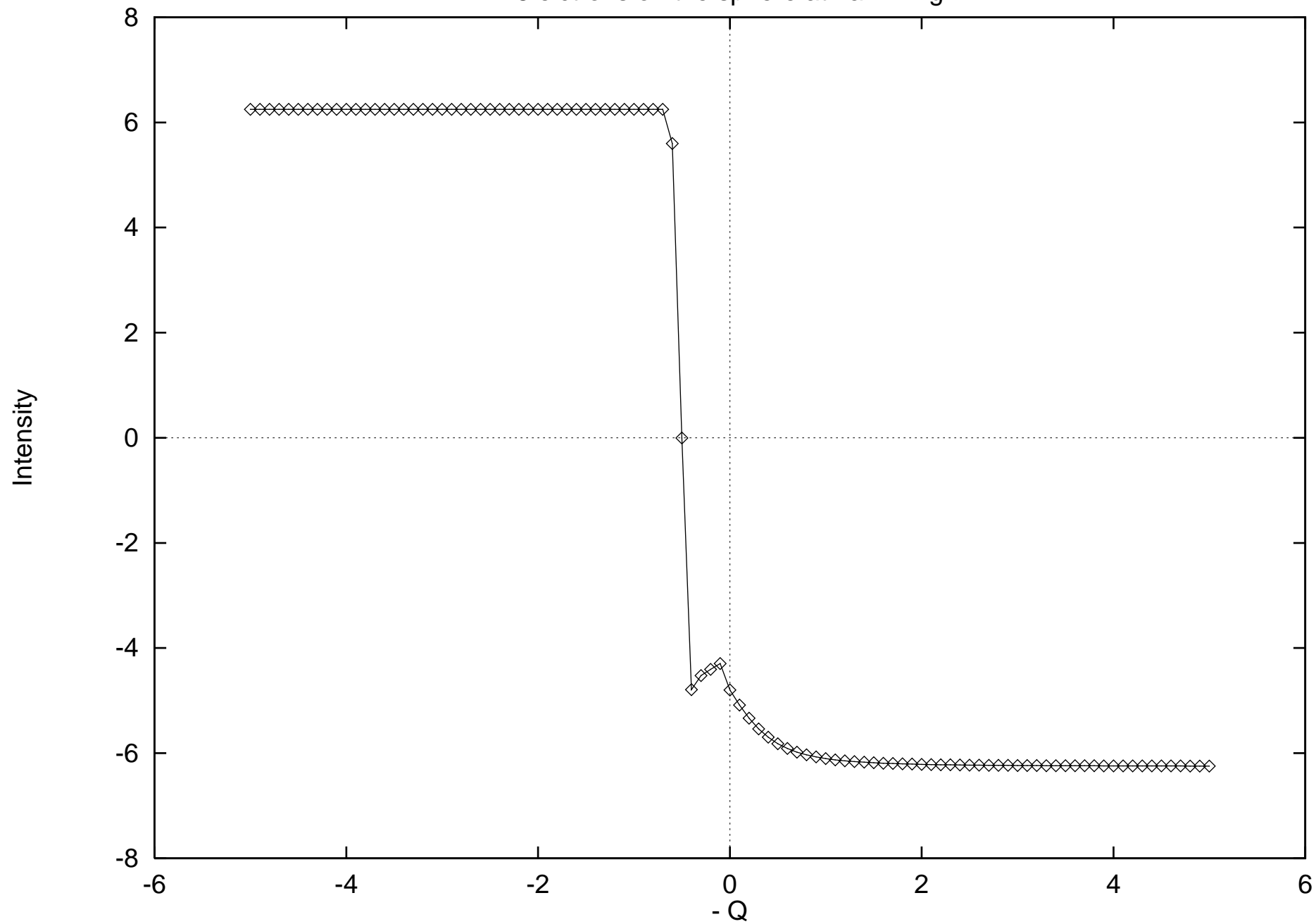


Flux through the ring with a parabolic well

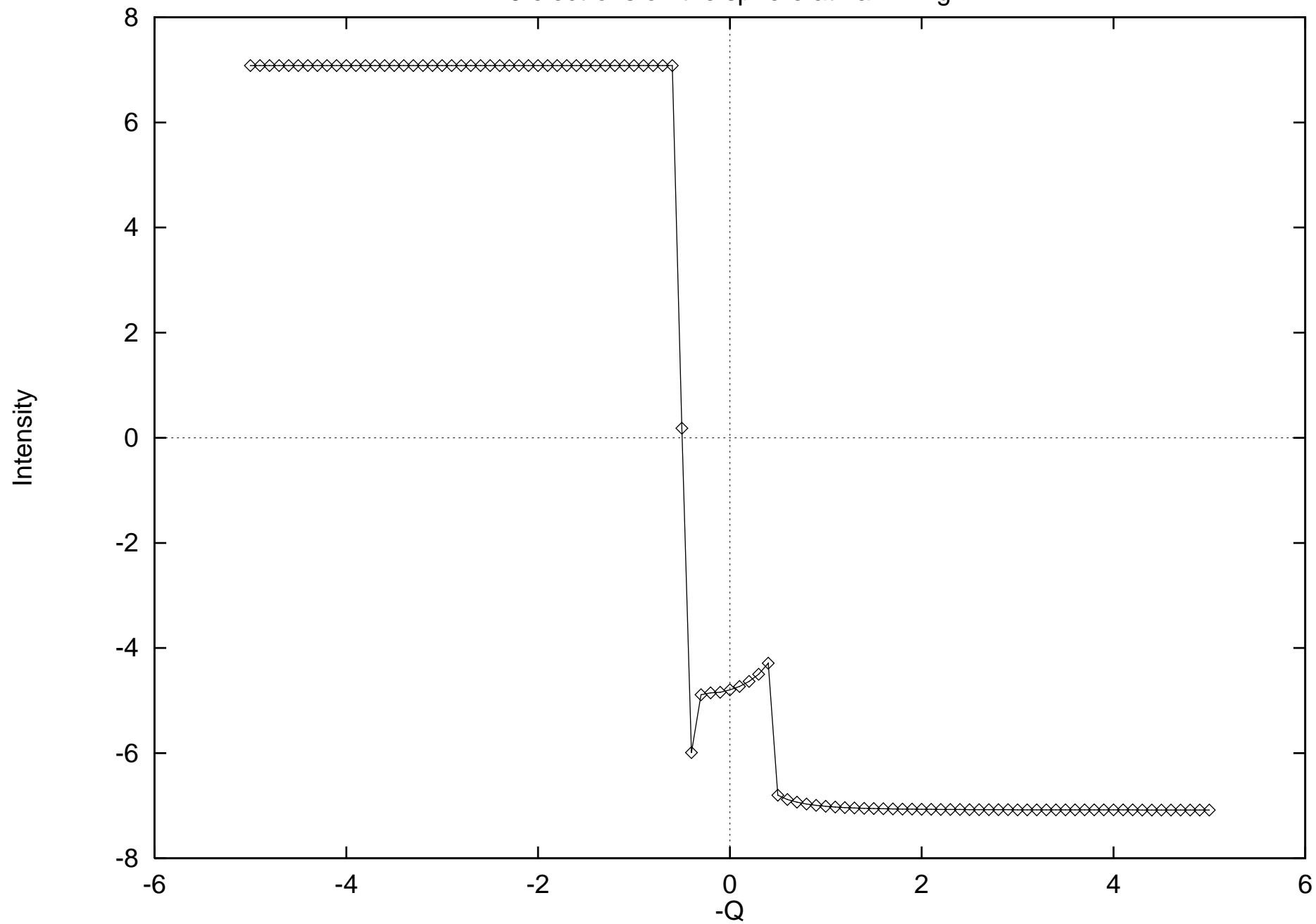




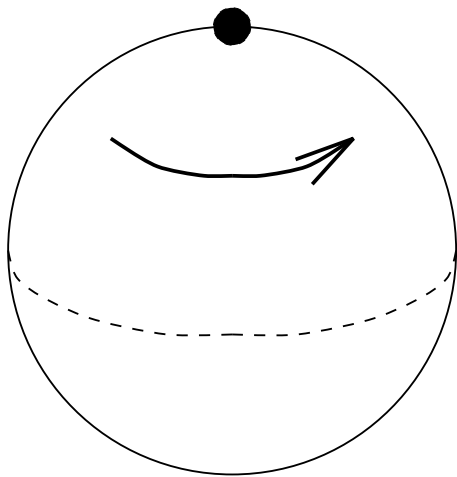
8 elctrons on the sphere at half filling



9 electrons on the sphere at half filling

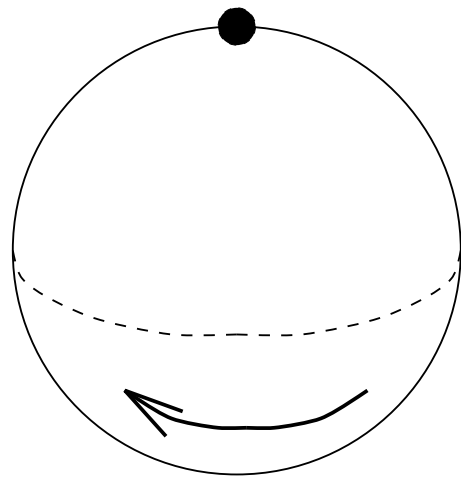


Large and positive charge



(a)

Large and negative charge



(b)